

Hierarchical graph sampling based minibatch learning with chain preservation and variance reduction

Qia Hu^{1,2†},

Bo Jiao^{1*†}

hqqqq@stu.xmu.edu.cn

jiaobleetc@outlook.com

¹Key Laboratory of Intelligent Manufacturing and Industrial Internet Technology,
Fujian Province University, Xiamen University Tan Kah Kee College, Zhangzhou, 363123, Fujian, China.
²School of Informatics, Xiamen University, Xiamen, 361102, Fujian, China.

Abstract: Graph sampling based Graph Convolutional Networks (GCNs) decouple the sampling from the forward and backward propagation during minibatch training, which exhibit good scalability in terms of layer depth and graph size. We propose HIS_{GCNs}, a hierarchical importance graph sampling based learning method. By constructing minibatches using sampled subgraphs, HIS_{GCNs} gives attention to the importance of both core and periphery nodes/edges in a scale-free training graph. Specifically, it preserves the centrum of the core to most minibatches, which maintains connectivity between periphery nodes, and samples periphery edges without core node interference, in order to keep more long chains composed entirely of low-degree nodes in the same minibatch. HIS_{GCNs} can maximize the discrete Ricci curvature (i.e., Ollivier-Ricci curvatures) of the edges in a subgraph that enables the preservation of important chains for information propagation, and can achieve a low node embedding variance and a high convergence speed. Diverse experiments on Graph Neural Networks (GNNs) with node classification tasks confirm superior performance of HIS_{GCNs} in both accuracy and training time.

Key Words: Graph convolutional network; Minibatch learning; Sampling; Discrete Ricci curvature.

1 Introduction

Graph Convolutional Networks (GCNs) perform efficient feature extraction and aggregation on attributed graphs [1]. However, with increasing scale of the graphs [2], GCNs face challenges in terms of computation and storage complexity. One prominent issue is known as “neighbor explosion” [3,4]. In a GCN, feature to be gathered for a node comes from its neighbors in the previous layer, and each of these neighbors recursively gathers feature from its previous layer. For a scale-free graph with low diameter, the expansion of the neighborhood for a single node quickly fills up a large portion of the graph, even with a small batch size [5,6]. Graph sampling based GCNs resolve the “neighbor explosion” by building every GCN on a subgraph with small size [2,6].

Graph sampling based GCNs first extract n subgraphs to construct minibatches, and then built a full GCN for each minibatch on a subgraph, which also brings new challenges in training, such as bias to nodes frequently sampled and loss of long chains that help propagate long-distance features. To alleviate these issues, loss normalization is an important technology [6], while preserving more critical chains in the same subgraph is indispensable, especially for long chains composed entirely of low-degree nodes, because 1. Chains with length not less than two represent the correlation between edges, and 2. Two connected nodes that have few neighbors are likely to be influential to each other [6]. Thus, we investigate a hierarchical importance graph sampling with the goal of reducing node aggregation variance while preserving more critical long chains in the same subgraph.

Many graphs are scale-free, such as social, collaboration and biological networks. The topology of these graphs has a core-periphery structure caused by preferential attachment [7], which attaches

* Corresponding author.

† These authors contributed equally to this work.

each newly-added node preferentially to high-degree nodes. Specifically, the structure is composed of a dense core with a few high-degree nodes and a sparse periphery with massive low-degree nodes [8-12]. Based on preferential attachment, as graph scale increases, internal connections of small and dense core are relatively stable, while the number of periphery nodes and their edges connecting to the core grow rapidly. Thus, preserving centrum structure of the small core is helpful in maintaining connection of subgraphs with small size [12]. Periphery is sparse, but its node number is large, resulting in a large number of long chains being contained within it. These chains composed entirely of low-degree nodes are critical for feature propagation [6]. Thus, a complete chain mentioned above should be preserved as much as possible in the same minibatch, even with a small size. The training of GCNs relies on many minibatches, all of which help alleviate information loss of these critical chains. Core-periphery structure enables each minibatch to simultaneously achieve two points: one is to preserve the core centrum to maintain connectivity, and the other is to preserve the peripheral long chains without core node interference. Therefore, we design a graph sampling based learning method HIS_{GCNs} using the hierarchical core-periphery structure.

Our contributions are summarized as follows: 1. We propose a hierarchical importance graph sampling based GCN minibatch learning method HIS_{GCNs}, objective to preserve more critical long chains in the same minibatch and reduce node aggregation variance, 2. We perform theoretical and experimental analysis of chain preservation and variance reduction in minibatch training, and 3. We validate the effectiveness of HIS_{GCNs} through extensive experiments on semi-supervised node classification tasks across various datasets, demonstrating its superior performance in both accuracy and training time. Open sourced code: <https://github.com/HuQiaCHN/HIS-GCN>.

The structure of this paper is organized as follows: Section 2 introduces related work, Section 3 provides design principles, Section 4 describes implementation detail of HIS_{GCNs}, and Section 5 validates the effectiveness of chain preservation and variance reduction and demonstrates superior performance of HIS_{GCNs} in both accuracy and training time.

2 Related work

2.1 GCN framework

GCNs extend convolution operations to graph-structured data, and propagate information between nodes in a graph [1-6]. For an un-directed, attributed graph $G = (\mathcal{V}, \mathcal{E})$ with nodes $v \in \mathcal{V}$ and edges $(u, v) \in \mathcal{E}$, where the number of nodes is $|\mathcal{V}| = N$ and the number of edges is $|\mathcal{E}|$. Each node in the graph is represented by a feature vector of length f . Then, an adjacency matrix $A \in \mathbb{R}^{N \times N}$ and a feature matrix $X \in \mathbb{R}^{N \times f}$ can be defined, where $A_{u,v} = 1$ if there is an edge between nodes u and v , and 0 otherwise, and the i^{th} row of X represents the feature vector of node v_i . Let $\hat{A} = \tilde{D}^{-1/2} \tilde{A} \tilde{D}^{-1/2}$, where $\tilde{A} = A + I_N$, I_N is an identity matrix, and \tilde{D} is the diagonal degree matrix of \tilde{A} with $\tilde{D}_{ii} = \sum_j \tilde{A}_{ij}$. Let $W^{(l)} \in \mathbb{R}^{f^{(l)} \times f^{(l+1)}}$ be the trainable weight matrix at layer l , σ be the activation function, and $H^{(l)} \in \mathbb{R}^{N \times f^{(l)}}$ be the node embedding matrix at layer l with $H^{(0)} = X$. Then, the architecture of GCNs may be summarized by the following expression:

$$H^{(l+1)} = \sigma(\hat{A} H^{(l)} W^{(l)}) \quad (1)$$

Let $\hat{A}_{v,u} \in \mathbb{R}$ be an element of \hat{A} , and $H^{(l)}(v) \in \mathbb{R}^{f^{(l)}}$ be the feature vector of node v at layer l . Then, GCNs can be interpreted by a message-passing framework, where each node passes information to its neighboring nodes (the activation function is omitted):

$$H^{(l+1)}(v) = \sum_{u \in \mathcal{V}} \hat{A}_{v,u} H^{(l)}(u) W^{(l)}, v \in \mathcal{V} \quad (2)$$

GCNs recursively aggregate information over multiple layers to generate representative feature vectors for each node, performing well in tasks like node classification. However, the computational complexity of Eq. (1) is $O(|\mathcal{E}|f^{(l)}f^{(l+1)})$ that makes GCN training slow for large or dense graphs. Additionally, both forward and backward propagation recursively expand node neighbors, which requires all nodes and edges to be loaded into memory, resulting in huge memory requirement. A potential solution is to sample the training graph to reduce its scale, thereby reducing computational and memory complexity [2-6,13-25].

2.2 Sampling-based graph learning

2.2.1 Node-wise sampling methods

Node-wise sampling methods extract a subset of nodes and their neighbors in each convolution layer to reduce computational complexity. A representative method is GraphSAGE [3], which generates node embeddings by randomly sampling a subset of k -hop neighbors, thus alleviating the issue of exponentially growing neighbors. Research [15] combines efficient random walks and graph convolutions to generate embeddings of nodes that incorporate both graph structure as well as node feature information. Research [16] extends GraphSAGE by limiting only two neighbors of each node to be sampled and using historical activations to reduce variance. These methods reduce memory demand by sampling neighbors, and re-sample the neighbors for each forward propagation.

2.2.2 Layer-wise sampling methods

Layer-wise sampling methods are improvements over node-wise samplings. Instead of sampling neighbors for each node, these methods sample a fixed number of nodes in each convolution layer to further reduce computational complexity. A representative method is FastGCN [17] that executes independent batch sampling of nodes in each layer to address the exponential growth of neighbors with increasing layers. To address the issue of broken connectivity caused by independent sampling across layers, some inter-layer dependence models have been proposed. Research [18] designs a top-down sequential model, in which the sampling in lower layers depends on the results of higher layers. Research [19] designs a layer-dependent importance sampling model that ensures connectivity between sampled nodes. Owing to the inter-layer dependence in sampling, these models incur additional time cost associated with sampling.

2.2.3 Graph sampling based methods

Graph sampling based methods create many minibatches, each built on a subgraph that is composed of some nodes and edges extracted from the same large-scale graph, and then train GCN on each of these minibatches and normalize correlation loss between different subgraphs. Cluster-GCN [20] partitions the graph into multiple clusters, and randomly combines a fixed number of clusters to a subgraph. RWT [2] samples subgraphs from the graph to constitute a mini-batch, and a full GNN is updated based on the mini-batch gradient. GraphSAINT [6] samples the graph using lightweight algorithms, such as importance based random node/edge, random walks and multi-dimensional random walks, and then uses normalization techniques to balance the frequency of sampled nodes and edges across different subgraphs. SHADOW-GNN [21] decouples the depth and scope of GNNs to improve expressivity and scalability without modifying layer architecture, where the scope is related to a shallow subgraph. BNS-GCN [22] considers the cost of data transfer between GPU and CPU for boundary nodes of different subgraphs and designs a random sampling for the nodes to reduce this overhead. IANS [23] adopts an improved adaptive neighbor sampling to form k subgraphs starting with k central nodes and defines a subgraph contrastive loss. GNN-LS [24] studies end-to-end learning capability of deep network to realize gradient optimization and samples nodes with an unfixed

probability. LoCur [25] extracts subgraphs through combinatorial sampling proportional to localized curvatures with 3-cycles, and demonstrates that the curvatures exhibit small errors in local structures of sparse training graphs. Owing to scalability in terms of layer depth and graph size, these methods exhibit high training efficiency on large-scale graphs [2,6,20-25].

Not extracting only one subgraph with small size, the graph sampling based methods extract many subgraphs for training, thus probability models are important in alleviating loss when propagating within and between subgraphs [2,25]. LoCur [25] interprets the node and edge samplers of GraphSAINT [6] as probability samplings proportional to the localized curvatures without a cycle (or 3-cycle), theoretically provides error bound of the localized curvatures with 3-cycles on Erdős-Rényi random graphs [26]. Although there could be a method that is more effected scale-free graphs than on mesh grid or Erdős-Rényi random graphs, LoCur [25] exhibits superior performance in various experiments even considering computational cost. Our method HIS_{G_{CN}s} adopts the framework as like [2,6,25], and focuses on the core-periphery structure unique to scale-free training graphs. The structure caused by preferential attachment [7] helps to preserve critical long chains.

3 Design principle

We design a graph sampling based minibatch learning method HIS_{G_{CN}s} that extracts many subgraphs for information propagation and reduces the variance of node feature aggregation. Our goal is different from the goal of graph sampling in fields of network crawling and visualization, which extracts only one subgraph to represent a given large-scale graph and reduces the variance of degree property [11,12]. To alleviate correlation loss between different subgraphs, HIS_{G_{CN}s} adopts the loss normalization technique of GraphSAINT [6] that eliminate bias to nodes more frequently sampled and incur little overhead in training time. HIS_{G_{CN}s} focuses on the preservation of important chains in the same subgraph, since these chains characterize complex edge correlations and are helpful in reducing the variance of node feature aggregation.

According to the subgraph-based training framework [2,6,25] and the above-mentioned motivation, we design HIS_{G_{CN}s} based on the following principles:

P1: Using degree threshold to partition core and periphery, objective to maximize the number of edges each of which connects a core node and a periphery node [12].

Nodes with degrees larger than the threshold are classified into core, while others are classified into periphery. The above-mentioned maximization method can significantly reduce the number of core nodes, which helps to preserve centrum structure of the core to most subgraphs without affecting the diversity of long chains in different subgraphs. Since node degree is a simple property, the threshold partition incurs little overhead in training time (see **Appendix B.1**).

P2: Using traversal-based and importance samplings to create the periphery of each subgraph.

Although the periphery of the large-scale training graph is sparse, the large number of periphery nodes results in significant impact of edges between low-degree nodes on training. In addition, two connected nodes that have few neighbors are likely to be influential to each other [6]. Thus, without core node interference, traversal-based samplings can preserve more and longer chains that are composed entirely of low-degree nodes in the same subgraph. Traditional traversal-based samplings start by a random seed, and then extract one or several neighbors of a node that has been traversed, until the expected fraction of nodes is collected [11,27-29]. HIS_{G_{CN}s} adopts these samplings in periphery construction of each subgraph, and designs an importance strategy for sampling next node from the neighbors of a traversed node objective to reduce node aggregation variance.

P3: With a distribution biased towards high-degree nodes, randomly choosing a fraction of core nodes from the neighbors of each periphery node that has been sampled by **P2**, and preserving all the chosen core nodes (removing duplicates) in subgraphs.

Periphery nodes are sparsely connected to each other but densely connected to core nodes in a scale-free graph [12], so that most periphery nodes have at least one core neighbor. Minibatches are constructed by many subgraphs with small size, thus the random choice of the core neighbors in **P3** is helpful in maintaining the diversity of chains. Removing core decomposes the scale-free training graph into many branches, thus the preservation of the centrum of the core is important for keeping the connectivity of subgraphs. Based on preferential attachment [7], the centrum nodes corresponding to a small number of core nodes with top-highest degrees are more easily connected by periphery nodes. Fig. 1 shows that there is a clear gap between the degrees of the centrum nodes and other marginal core nodes in large-scale training graphs. The biased random choice in **P3** is executed for each sampled periphery node, making it difficult for the centrum nodes connected by a large number of periphery nodes to fall outside the corresponding subgraph.

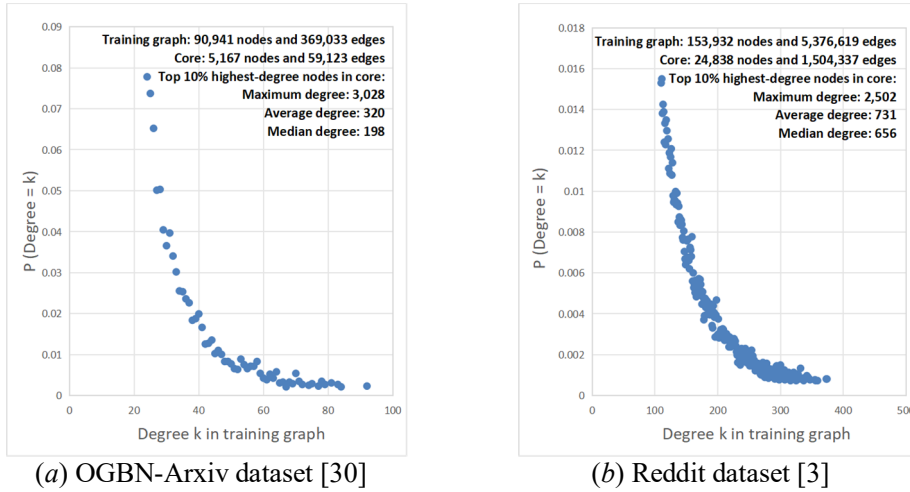


Figure 1. Degree distribution of core nodes in training graphs. $P(\text{Degree} = k)$ denotes the ratio of the number of core nodes with degree k to the number of core nodes. The maximum k value of the dots in (a)(b) is equal to the maximum degree of remaining nodes after removing top 10% highest-degree core nodes. The maximum, average and median degrees of the removed core nodes are listed in (a)(b). Centrum nodes are a small number of core nodes with top-highest degrees, and core nodes other than the centrum nodes are defined as marginal core nodes. The OGBN-Arxiv and Reddit datasets were split into training, validation and test sets (see **Table 1**).

P4: Preserving all edges between sampled nodes to the corresponding subgraph [6].

Based on **P2** and **P3**, sampling from neighbors of a sampled node can maximize the preservation of connections between two periphery nodes and between periphery and core nodes. In addition, the core nodes of a scale-free graph, especially the centrum nodes, are densely interconnected [12], thus **P4** maintains the connectivity of each subgraph.

HIS_{GCNs} samples from periphery to core, avoiding the high uncertainty of randomly extracting next node from neighbors of a centrum node of the core, since the number of the neighbors in large-scale training graphs is very large, as shown in Fig. 1. Owing to the high uncertainty, HIS_{GCNs} does not view the centrum node as the starting or ending point of information propagation, but only uses it to shorten the length of the propagation path. As shown in Fig. 2, HIS_{GCNs} can preserve more and longer chains in periphery, and make each subgraph more connected through a few centrum nodes.

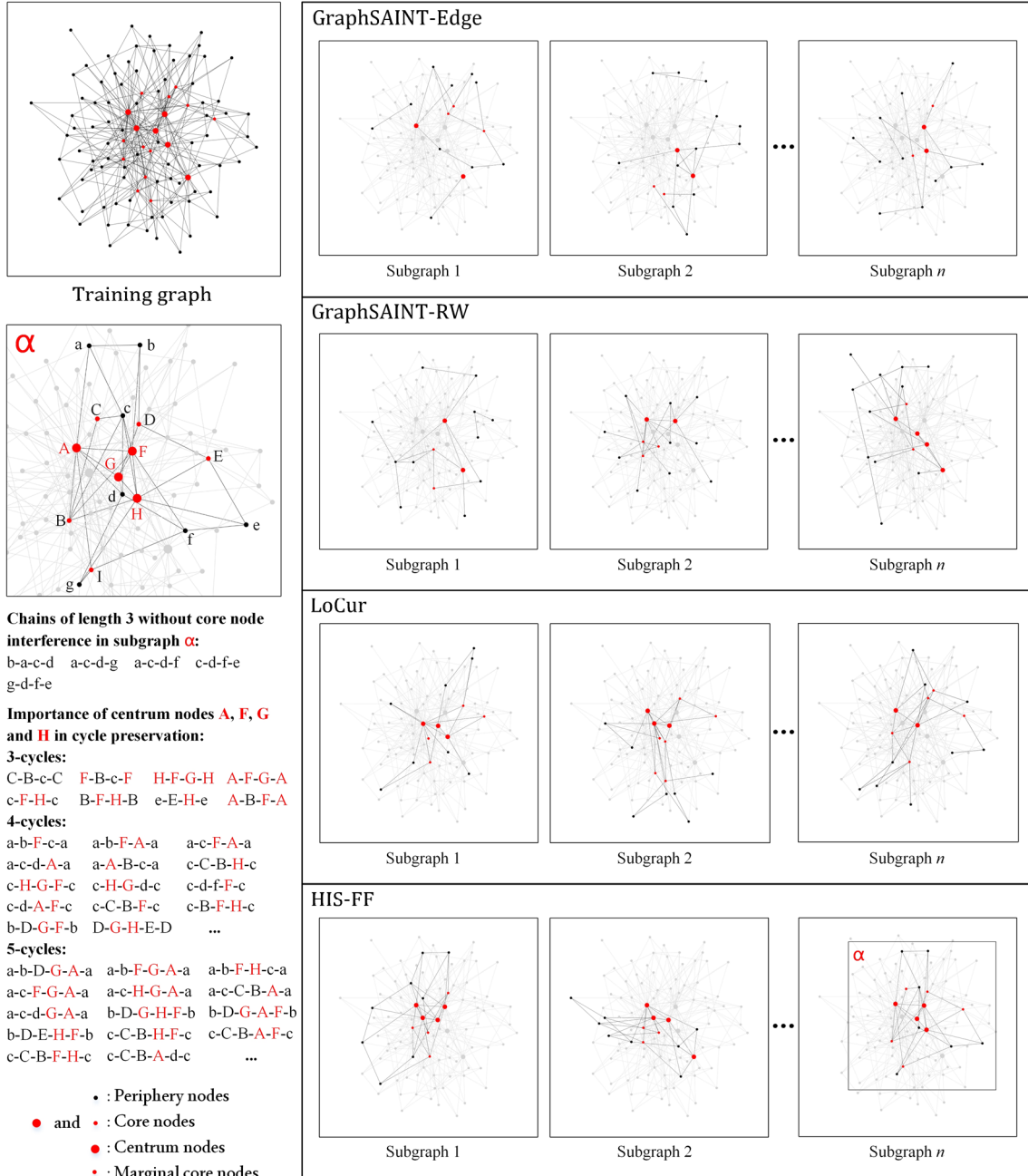


Figure 2. Sample examples on a training graph with 100 nodes, in which red and black respectively represent core and periphery nodes. The training graph is generated by Barabasi-Albert (BA) model [7]. Based on **P1**, the degree threshold of the small-scale BA graph is 7, thus nodes with degrees larger than 7 in the graph are marked in red, while others are marked in black. GraphSAINT-Edge is an edge sampler [6] with $p_{u,v} \propto 1/d_u + 1/d_v$ where $p_{u,v}$ is the probability of sampling edge (u, v) and d_u, d_v denote node degrees. A subgraph is induced by nodes that are end-points of the sampled edges. GraphSAINT-RW is a random walk sampler [6] that first samples r root nodes uniformly at random and then r walkers respectively start from one of the root nodes and each of them goes h hops (the sampler outputs a node induced subgraph). LoCur [25] starts at some initial nodes, and then extends to neighboring nodes to maximize the sum of localized curvatures of edges (the localized curvatures are illustrated in **Definition 1**). HIS-FF is one of our HIS_{G_{CN}s} samplers that meet **P1** to **P4** and are designed in Section 4. Because only the topology of the BA graph is considered, the 2-norm of the feature vector, i.e., $\|X(v)\|$, for each $v \in \mathcal{V}$ is set as 1. Sample size defined as the number of nodes in the subgraphs is set as 15; however, owing to randomness and the removal of duplicate nodes, the actual sample size usually has a deviation of 1 to 2. Note that partial edges overlap in the graph visualization.

Owing to the large number of neighbors of a centrum node, the influence from a peripheral node (or a marginal core node) that falls in the neighbors to the centrum node is relatively small. However, if two low-degree nodes are attached to the same centrum node, they usually have some similar features. As shown in Fig. 3, the centrum nodes play an important role in establishing correlations between different convolutional layers. Note that the training graph in Fig. 2 only has 100 nodes, resulting in a slight degree difference between centrum and marginal core nodes, but this difference is significantly amplified on large-scale graphs, as shown in Fig. 1. In addition, by comparing Figs. 1 and 2, we observe that the ratio of the number of centrum nodes to the total number of nodes in large-scale graphs can be further reduced.

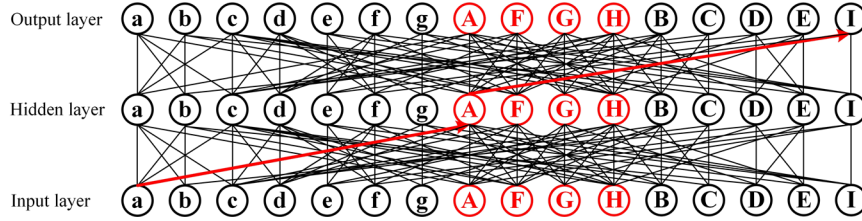


Figure 3. Two-layer GCN on subgraph α in left side of Fig. 2. Centrum node A shortens the path length between periphery node a and marginal core node I, establishing correlations between different convolutional layers.

Definition 1. (Localized Curvature with 3-cycles [25]) d_x and d_y denote the degrees of nodes x and y , respectively. $\Delta_{\#}(x, y)$ represents the number of triangles (3-cycles) including edge (x, y) . $d_x \wedge d_y$ and $d_x \vee d_y$ denote $\min[d_x, d_y]$ and $\max[d_x, d_y]$, respectively. $(\cdot)_+$ is defined as $\max[\cdot, 0]$. Then, localized curvature κ_{xy} for edge (x, y) has the following lower bound:

$$\kappa_{xy} \geq -\left(1 - \frac{1}{d_x} - \frac{1}{d_y} - \frac{\Delta_{\#}(x, y)}{d_x \wedge d_y}\right)_+ - \left(1 - \frac{1}{d_x} - \frac{1}{d_y} - \frac{\Delta_{\#}(x, y)}{d_x \vee d_y}\right)_+ + \frac{\Delta_{\#}(x, y)}{d_x \vee d_y} \quad (3)$$

The lower bound of κ_{xy} in Eq. (3) can be considered the localized curvature for the Ollivier-Ricci curvature [31,32] that considers random walk-based probability measures with Markov chain and 1-Wasserstein transportation distance (see **Appendix A**). The large curvature κ_{xy} indicates the small distance between the probability measures for two nodes x and y .

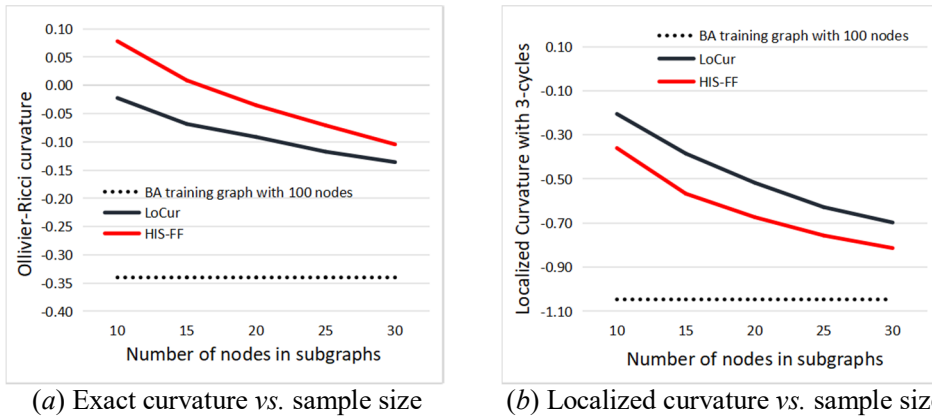


Figure 4. Comparison of Ollivier-Ricci and localized curvatures using the BA training graph with 100 nodes in Fig. 2. The curvatures of LoCur and HIS-FF were evaluated using the average value of edge curvatures of 500 subgraphs for each sample size (i.e., the number of nodes in subgraphs).

The curvature of an edge refers to its curvature on the training graph, not on a subgraph.

Subgraph sampling that maximizes the edge curvatures amounts to minimizing the distributional difference between the training graph and subgraph [25].

LoCur samples subgraphs to maximize the localized curvature [25]. According to Eq. (3), the lower bound of κ_{xy} grows with decreasing d_x , d_y and increasing $\Delta_{\#}(x, y)$. Thus, high curvature edges appear in two instances: one is the edges connecting two low-degree nodes, and the other is the edges that are included in plenty of cycles with small length. **P1** to **P4** makes HIS_{G_{CN}s} satisfy: 1. Preserving peripheral long chains without core node interference, 2. Preserving core centrum nodes to most subgraphs, and 3. Preserving all edges between sampled nodes. The peripheral long chains are composed of the edges connecting low-degree nodes. In scale-free graphs, periphery nodes are densely connected to core nodes (especially a few centrum nodes), and the core nodes are densely interconnected [12], that is, the edges connecting two low-degree periphery nodes are prone to falling into cycles passing through at least one centrum node. In addition, the dense centrum includes a large number of cycles with small length. As shown in left side of Fig. 2, we list two types of chain instances: one represents deep information propagation along low-degree nodes (without core node interference), and the other shows the role of centrum nodes in preserving cycles that shorten the length of propagation paths between periphery or marginal core nodes. Experiments in Fig. 4 show that HIS_{G_{CN}s} and LoCur [25] have the same goal of maximizing the curvatures.

4 Proposed method: HIS_{G_{CN}s}

4.1 Core-periphery partition

Based on **P1**, we adopt the method in [12] that defines a degree threshold d_{th} to partition core and periphery in scale-free training graph $G = (\mathcal{V}, \mathcal{E})$ with node set \mathcal{V} and edge set \mathcal{E} .

$$d_{th} = \operatorname{argmax}_d |\{(u, v) \in \mathcal{E} \mid u, v \in \mathcal{V}, d_u > d, d_v \leq d\}| \quad (4)$$

where d_u and d_v respectively denote the degrees of nodes u and v in graph G , and $|\cdot|$ is defined as the cardinality of a set. Then, G is partitioned into a small and dense core $G_{cor} = (\mathcal{V}_{cor}, \mathcal{E}_{cor})$, a large and sparse periphery $G_{per} = (\mathcal{V}_{per}, \mathcal{E}_{per})$, and a vertical edge set \mathcal{E}_{ver} :

$$\mathcal{V}_{cor} = \{v \in \mathcal{V} \mid d_v > d_{th}\}, \quad \mathcal{E}_{cor} = \{(u, v) \in \mathcal{E} \mid u, v \in \mathcal{V}_{cor}\} \quad (5)$$

$$\mathcal{V}_{per} = \{v \in \mathcal{V} \mid d_v \leq d_{th}\}, \quad \mathcal{E}_{per} = \{(u, v) \in \mathcal{E} \mid u, v \in \mathcal{V}_{per}\} \quad (6)$$

$$\mathcal{E}_{ver} = \{(u, v) \in \mathcal{E} \mid u \in \mathcal{V}_{cor}, v \in \mathcal{V}_{per}\} \quad (7)$$

In scale-free graph G , the probability of randomly selecting a k -degree node decays as a power law $P(k) \propto k^{-\tau}$, where τ is the degree exponent [7]. That is, a large number of low-degree nodes exist in G_{per} . Thus, we can increase the degree threshold d_{th} from 1 with steplength 1 until Eq. (4) is satisfied [12]. There are two advantages of the degree threshold partition: one is to minimize the number of nodes in G_{cor} , and the other is that its overhead is small (see **Appendix B.1**).

4.2 Hierarchical importance sampling

We derive samplers for reducing the variance of node information aggregation in Eq. (2). Based on **P2**, during the process of traversing neighbors in the periphery, we define $p(u \mid v)$ as the probability of sampling $u \in \mathcal{V}_{per}$ from the neighbors of a given traversed periphery node v . In addition, based on **P3**, during the process of choosing core neighbors, we define $q(u' \mid v)$ as the probability of sampling $u' \in \mathcal{V}_{cor}$ from the neighbors of a given sampled periphery node v .

The defined probabilities meet the following constraints:

$$\sum_{u \in \mathcal{V}_{per}} p(u \mid v) = 1, \quad \sum_{u' \in \mathcal{V}_{cor}} q(u' \mid v) = 1 \quad (8)$$

To derive $p(u | v)$, we use a theoretical method under the assumption of layer independence. This is similar to the treatment of layers independently by prior work [6,17,18]. To obtain $q(u' | v)$, we rely on the empirical analysis on centrum nodes in Section 3, that is, the centrum nodes play an important role in preserving cycles that are entangled with peripheral long chains and establishing complex correlations across different layers. The effectiveness of variance reduction for the empirical analysis will be validated in Section 5.3.

Under the assumption of layer independence, based on Eq. (2), we transform the embedding of a periphery node v at layer $l + 1$ as follows:

$$H^{(l+1)}(v) = \left(\sum_{u \in \mathcal{V}_{per}} \hat{A}_{v,u} H^{(l)}(u) + \sum_{u' \in \mathcal{V}_{cor}} \hat{A}_{v,u'} H^{(l)}(u') \right) W^{(l)} \quad (9)$$

The vast majority of nodes in the scale-free training graph are allocated to the periphery, thus Eq. (9) only considers the embedding of nodes in the periphery.

Based on Eq. (8), we derive two expectation forms:

$$\mu_{per}(v) = \mathbb{E}_{p(u|v)} \left[\frac{1}{p(u | v)} \hat{A}_{v,u} H^{(l)}(u) \right] = \sum_{u \in \mathcal{V}_{per}} \left[\frac{1}{p(u | v)} \hat{A}_{v,u} H^{(l)}(u) \cdot p(u | v) \right] \quad (10)$$

$$\mu_{cor}(v) = \mathbb{E}_{q(u'|v)} \left[\frac{1}{q(u' | v)} \hat{A}_{v,u'} H^{(l)}(u') \right] = \sum_{u' \in \mathcal{V}_{cor}} \left[\frac{1}{q(u' | v)} \hat{A}_{v,u'} H^{(l)}(u') \cdot q(u' | v) \right] \quad (11)$$

Based on Eqs. (10) and (11), we transform Eq.(9) to the following form:

$$H^{(l+1)}(v) = (\mu_{per}(v) + \mu_{cor}(v)) W^{(l)} \quad (12)$$

We evaluate the expectations $\mu_{per}(v)$ and $\mu_{cor}(v)$ using Monte Carlo sampling [16,43,44]:

$$\hat{\mu}_{per}(v) = \frac{1}{n} \sum_{i=1}^n \frac{1}{p(u_i | v)} \hat{A}_{v,u_i} H^{(l)}(u_i), \quad u_i \sim p(u | v) \quad (13)$$

$$\hat{\mu}_{cor}(v) = \frac{1}{n} \sum_{i=1}^n \frac{1}{q(u'_i | v)} \hat{A}_{v,u'_i} H^{(l)}(u'_i), \quad u'_i \sim q(u' | v) \quad (14)$$

Like research [6], we first assume that $H^{(l)}(u_i)$ is one dimensional (i.e., a scalar), $i = 1, 2, \dots, n$. Now, we derive the variance of Eq. (13) and calculate $p(u | v)$ that minimizes the variance.

$$Var[\hat{\mu}_{per}(v)] = \mathbb{E}_{p(u|v)} \left[\left(\frac{1}{n} \sum_{i=1}^n \frac{1}{p(u_i | v)} \hat{A}_{v,u_i} H^{(l)}(u_i) \right)^2 \right] - [\mu_{per}(v)]^2 \quad (15)$$

Based on iid samples $u_1, u_2, \dots, u_n \sim p(u | v)$, Eq. (8) and Eq. (10), we can derive:

$$\begin{aligned} \mathbb{E}_{p(u|v)} \left[\left(\frac{1}{n} \sum_{i=1}^n \frac{1}{p(u_i | v)} \hat{A}_{v,u_i} H^{(l)}(u_i) \right)^2 \right] &= \mathbb{E}_{p(u|v)} \left[\left(\frac{1}{n} \sum_{i=1}^n \frac{1}{p(u_i | v)} \hat{A}_{v,u_i} H^{(l)}(u_i) \right) \left(\frac{1}{n} \sum_{j=1}^n \frac{1}{p(u_j | v)} \hat{A}_{v,u_j} H^{(l)}(u_j) \right) \right] \\ &= \mathbb{E}_{p(u|v)} \left[\frac{1}{n^2} \sum_{i=1}^n \sum_{j=1}^n \frac{1}{p(u_i | v)} \hat{A}_{v,u_i} H^{(l)}(u_i) \frac{1}{p(u_j | v)} \hat{A}_{v,u_j} H^{(l)}(u_j) \right] \\ &= \frac{1}{n^2} \sum_{i=1}^n \mathbb{E}_{p(u_i|v)} \left[\frac{1}{p(u_i | v)} \hat{A}_{v,u_i} H^{(l)}(u_i) \right]^2 \\ &\quad + \frac{2}{n^2} \sum_{i=1}^{n-1} \sum_{j=i+1}^n \left\{ \mathbb{E}_{p(u_i|v)} \left[\frac{1}{p(u_i | v)} \hat{A}_{v,u_i} H^{(l)}(u_i) \right] \cdot \mathbb{E}_{p(u_j|v)} \left[\frac{1}{p(u_j | v)} \hat{A}_{v,u_j} H^{(l)}(u_j) \right] \right\} \\ &= \frac{1}{n} \mathbb{E}_{p(u|v)} \left[\frac{1}{p(u | v)} \hat{A}_{v,u} H^{(l)}(u) \right]^2 + \left(1 - \frac{1}{n} \right) \left\{ \mathbb{E}_{p(u|v)} \left[\frac{1}{p(u | v)} \hat{A}_{v,u} H^{(l)}(u) \right] \right\}^2 \\ &= \frac{1}{n} \sum_{u \in \mathcal{V}_{per}} \left\{ \left[\frac{1}{p(u | v)} \hat{A}_{v,u} H^{(l)}(u) \right]^2 \cdot p(u | v) \right\} + \left(1 - \frac{1}{n} \right) [\mu_{per}(v)]^2 \\ &= \frac{1}{n} \sum_{u \in \mathcal{V}_{per}} \left[\frac{1}{p(u | v)} \hat{A}_{v,u}^2 |H^{(l)}(u)|^2 \right] + \left(1 - \frac{1}{n} \right) [\mu_{per}(v)]^2 \end{aligned}$$

Thus, we transform Eq. (15) to the following form:

$$\text{Var}[\hat{\mu}_{per}(v)] = \frac{1}{n} \sum_{u \in \mathcal{V}_{per}} \left[\frac{1}{p(u|v)} \hat{A}_{v,u}^2 |H^{(l)}(u)|^2 \right] - \frac{1}{n} [\mu_{per}(v)]^2 \quad (16)$$

Based on Eq.(10), we transform Eq. (16) to the following form:

$$\text{Var}[\hat{\mu}_{per}(v)] = \frac{1}{n} \sum_{u \in \mathcal{V}_{per}} \left[\frac{1}{p(u|v)} \hat{A}_{v,u}^2 |H^{(l)}(u)|^2 \right] - \frac{1}{n} \left[\sum_{u \in \mathcal{V}_{per}} \hat{A}_{v,u} H^{(l)}(u) \right]^2 \quad (17)$$

Eq. (8) shows that $\sum_{u \in \mathcal{V}_{per}} p(u|v) = 1$. By Cauchy-Schwarz inequality:

$$\sum_{u \in \mathcal{V}_{per}} \left[\frac{1}{p(u|v)} \hat{A}_{v,u}^2 |H^{(l)}(u)|^2 \right] \sum_{u \in \mathcal{V}_{per}} p(u|v) = \sum_{u \in \mathcal{V}_{per}} \left[\frac{\hat{A}_{v,u} |H^{(l)}(u)|}{\sqrt{p(u|v)}} \right]^2 \sum_{u \in \mathcal{V}_{per}} (\sqrt{p(u|v)})^2 \geq \left[\sum_{u \in \mathcal{V}_{per}} \hat{A}_{v,u} |H^{(l)}(u)| \right]^2$$

The equality is achieved when $\frac{\hat{A}_{v,u} |H^{(l)}(u)|}{\sqrt{p(u|v)}} \propto \sqrt{p(u|v)}$, i.e., variance is minimized when

$$p(u|v) \propto \hat{A}_{v,u} |H^{(l)}(u)| \quad (18)$$

For multi-dimensional case of $H^{(l)}(u)$, following similar steps as above, it is easy to show that the optimal sampling probability to minimize the variance is:

$$p(u|v) \propto \hat{A}_{v,u} \|H^{(l)}(u)\| \quad (19)$$

where $\|\cdot\|$ denotes 2-norm with $\|(x_1, x_2, \dots, x_k)\| = (\sum_{i=1}^k x_i^2)^{1/2}$.

Like research [18], the initial feature vector $X(u)$ defined in Section 2.1 was used to approximate the hidden feature vector $H^{(l)}(u)$. Thus, Eq. (19) can be simplified as:

$$p(u|v) \propto \hat{A}_{v,u} \|X(u)\| \quad (20)$$

In GCNs of Section 2.1, $\hat{A}_{v,u} = 1/\sqrt{(d_v+1)(d_u+1)}$, where d_v and d_u denote the degrees of nodes v and u , respectively. Since v is a given node, $\hat{A}_{v,u} \propto 1/\sqrt{d_u+1}$.

Thus, we transform Eq. (20) to the following form:

$$p(u|v) \propto \frac{\|X(u)\|}{\sqrt{d_u+1}} \quad (21)$$

Following similar steps as Eqs. (15) to (21), we derive $q(u'|v) \propto \|X(u')\|/\sqrt{d_{u'}+1}$ that **conflicts with P3**, since $q(u'|v)$ decreases with increasing $d_{u'}$ where $u' \in \mathcal{V}_{cor}$, but **P3** needs a probability distribution that is biased towards high-degree nodes. Similar to Eq. (17), we derive

$$\text{Var}[\hat{\mu}_{cor}(v)] = \frac{1}{n} \sum_{u' \in \mathcal{V}_{cor}} \left[\frac{1}{q(u'|v)} \hat{A}_{v,u'}^2 |H^{(l)}(u')|^2 \right] - \frac{1}{n} \left[\sum_{u' \in \mathcal{V}_{cor}} \hat{A}_{v,u'} H^{(l)}(u') \right]^2 \quad (22)$$

However, $\hat{A}_{v,u'} = 1/\sqrt{(d_v+1)(d_{u'}+1)}$ is very small for core node u' in Eq. (22), especially for centrum node u' , because the degree of the core node (especially for the centrum node) is obviously (or extremely) higher than that of a periphery node, as shown in Fig. 1. In addition, the percentage of core nodes in large scale-free graphs is usually very low, for example, the ratio of the number of core nodes to the number of total nodes is 5.68% ($\frac{5,167}{90,941}$) in Fig. 1(a) and 16.13% ($\frac{24,838}{153,932}$) in Fig. 1(b), respectively. That is, $|\mathcal{V}_{cor}| \ll |\mathcal{V}_{per}|$.

Therefore, based on Eqs. (12), (17) and (22), we observe that Eq. (22) can be viewed as noise in the analysis of variance theory. To derive $q(u'|v)$, we adopt the empirical analysis on centrum nodes in Section 3, that is, preserving the centrum in most subgraphs is important for HIS_{GCNs}. Thus, we empirically set $q(u'|v) \propto \hat{A}_{v,u'} \|X(u')\| (d_{u'}+1)$, namely

$$q(u'|v) \propto \|X(u')\| \sqrt{d_{u'}+1} \quad (23)$$

As is well known, $q(u' | v)$ in Eq. (23) is biased towards high-degree nodes u' .

4.3 Pseudo codes

A pre-processing, namely the core-periphery partition on the training graph, is executed before subgraph sampling. The pre-processing only runs once and incurs little time. To obtain n subgraphs, HIS_{G_{CN}s} adopts a traversal-based method that samples nodes in the periphery $G_{per} = (\mathcal{V}_{per}, \mathcal{E}_{per})$ without core node interference, and preserves a fraction of core neighbors for each newly-traversed periphery node, until the number of sampled periphery and core nodes satisfies desired sample size. The subgraphs preserve all edges between the sampled nodes. At each iteration, for a traversed periphery node v , HIS_{G_{CN}s} samples its periphery neighbors with $u_1, u_2, \dots, u_s \sim p(u | v)$ and its core neighbors with $u'_1, u'_2, \dots, u'_t \sim q(u' | v)$, where s is determined by the chosen traversal-based method and $t = \langle \gamma \cdot |\mathcal{N}_{cor}(u', v) \in \mathcal{E}_{ver}| \rangle$. Note that \mathcal{E}_{ver} is defined in Eq. (7) and $\langle \cdot \rangle$ rounds a scalar to the nearest integer. Parameter $\gamma \in (0, 1]$ decreases with growth of the scale of the training graph, since the degree difference between centrum and marginal core nodes is amplified on large scale-free graphs. We experimentally set $\gamma = 0.4$ for training graphs that have over 100,000 nodes, otherwise $\gamma = 1$. In this section, HIS_{G_{CN}s} updates two traversal-based methods, namely Forest Fire (FF) [28] and GraphSAINT-RW [6], and their pseudo codes are listed in Algorithms 1 and 2.

Algorithm 1: HIS-FF

Input: Scale-free training graph $G = (\mathcal{V}, \mathcal{E})$, core $G_{cor} = (\mathcal{V}_{cor}, \mathcal{E}_{cor})$, periphery $G_{per} = (\mathcal{V}_{per}, \mathcal{E}_{per})$, vertical edge set \mathcal{E}_{ver} , parameter γ , sample size \hat{n} .
Output: Subgraph $G_{sub} = (\mathcal{V}_{sub}, \mathcal{E}_{sub})$.

- 1: Initialize an empty FIFO (First-In First-Out) queue Q , $\mathcal{V}_{sub} \leftarrow \emptyset$.
- 2: **While** $|\mathcal{V}_{sub}| < \hat{n}$ **do**
- 3: **If** Q is empty, **then** uniformly at random choose a seed node $w \notin \mathcal{V}_{sub}$ from \mathcal{V}_{per} and add w to Q .
- 4: Extract and delete node v from Q , and update $\mathcal{V}_{sub} \leftarrow \mathcal{V}_{sub} \cup \{v\}$.
- 5: Sample $t = \langle \gamma \cdot |\mathcal{N}_{cor}(v)| \rangle$ nodes $u'_1, u'_2, \dots, u'_t \sim q(u' | v) = \|X(u')\| \sqrt{d_{u'} + 1} / \sum_{u' \in \mathcal{N}_{cor}(v)} \|X(u')\| \sqrt{d_{u'} + 1}$ from $\mathcal{N}_{cor}(v) = \{u' \in \mathcal{V}_{cor} | (u', v) \in \mathcal{E}_{ver}\}$, and update $\mathcal{V}_{sub} \leftarrow \mathcal{V}_{sub} \cup \{u'_1, u'_2, \dots, u'_t\}$.
- 6: Generate a random number $s \sim$ Geometric distribution with mean $(1 - p)^{-1}$, where p is experimentally set to 0.5.
 If $|\mathcal{V}_{sub}| + |Q| < \hat{n}$, **then** sample s nodes $u_1, u_2, \dots, u_s \sim p(u | v) = (\|X(u)\| / \sqrt{d_u + 1}) / \sum_{u \in \mathcal{N}_{per}(v)} (\|X(u)\| / \sqrt{d_u + 1})$ from $\mathcal{N}_{per}(v) = \{u \in \mathcal{V}_{per} | (u, v) \in \mathcal{E}_{per}, u \notin \mathcal{V}_{sub}, u \notin Q\}$, and add u_1, u_2, \dots, u_s to Q .
- 7: **End while** #Annotation: $|\mathcal{V}_{sub} \cup \{u'_1, u'_2, \dots, u'_t\}| \approx |\mathcal{V}_{sub}|$ in line 5, since many periphery nodes are connected to the same centrum node.
- 8: $G_{sub} = (\mathcal{V}_{sub}, \mathcal{E}_{sub}) \leftarrow$ Node induced subgraph of G from \mathcal{V}_{sub} .

Algorithm 2: HIS-RW

Input: Scale-free training graph $G = (\mathcal{V}, \mathcal{E})$, core $G_{cor} = (\mathcal{V}_{cor}, \mathcal{E}_{cor})$, periphery $G_{per} = (\mathcal{V}_{per}, \mathcal{E}_{per})$, vertical edge set \mathcal{E}_{ver} , parameter γ , sample size \hat{n} , walk length h .
Output: Subgraph $G_{sub} = (\mathcal{V}_{sub}, \mathcal{E}_{sub})$.

- 1: Initialize $\mathcal{V}_{sub} \leftarrow \emptyset$.
- 2: **While** $|\mathcal{V}_{sub}| < \hat{n}$ **do**
- 3: Uniformly at random choose a seed node v from \mathcal{V}_{per} .
- 4: **For** $d = 1$ to $h + 1$ **do**
- 5: **If** $v \notin \mathcal{V}_{sub}$, **then** sample $t = \langle \gamma \cdot |\mathcal{N}_{cor}(v)| \rangle$ nodes
 $u'_1, u'_2, \dots, u'_t \sim q(u' | v) = \|X(u')\| \sqrt{d_{u'} + 1} / \sum_{u' \in \mathcal{N}_{cor}(v)} \|X(u')\| \sqrt{d_{u'} + 1}$
 from $\mathcal{N}_{cor}(v) = \{u' \in \mathcal{V}_{cor} | (u', v) \in \mathcal{E}_{ver}\}$,
 update $\mathcal{V}_{sub} \leftarrow \mathcal{V}_{sub} \cup \{u'_1, u'_2, \dots, u'_t\}$, and update $\mathcal{V}_{sub} \leftarrow \mathcal{V}_{sub} \cup \{v\}$.
- 6: **If** $d < h + 1$, **then** sample a node $u_1 \sim p(u | v) = (\|X(u)\| / \sqrt{d_u + 1}) / \sum_{u \in \mathcal{N}_{per}(v)} (\|X(u)\| / \sqrt{d_u + 1})$
 from $\mathcal{N}_{per}(v) = \{u \in \mathcal{V}_{per} | (u, v) \in \mathcal{E}_{per}\}$,
 and update $v \leftarrow u_1$.
- 7: **End For**
- 8: **End while**
- 9: $G_{sub} = (\mathcal{V}_{sub}, \mathcal{E}_{sub}) \leftarrow$ Node induced subgraph of G from \mathcal{V}_{sub} .

5 Experiments

In this section, we experimentally validate the effectiveness of HIS-FF on chain/cycle preservation and variance reduction, and compare our method HIS_{G_{CN}s} with several baseline algorithms on classic graph datasets for semi-supervised node classification tasks. The training algorithm of our method HIS_{G_{CN}s} can be found in **Appendix C**. Experiments were conducted on a desktop computer equipped with a GPU 4070 and a 3.50 GHz 13th Gen Intel(R) Core(TM) i5-13600KF CPU, with 32GB of RAM and 16GB of GPU memory, and implemented in PyTorch and Python 3.

5.1 Graph datasets

We chose six scale-free datasets in Table 1 for node classification tasks. The datasets were split into training, validation and test sets. CiteSeer [33] and Pubmed [34] are two classical small-scale datasets that were split by the method in [17]. PPI-Large, i.e., an abbreviation of PPI (large version) [6], is a Protein-Protein Interaction network, Reddit [3] is a social network, OGBN-Arxiv [30] is a citation network, and OGBN-Products [30] is a product information network. The training, validation and test sets of PPI-Large, Reddit, OGBN-Arxiv and OGBN-Products have been split in the datasets. In addition, some graphs from Stanford large network dataset collection [35] were used for the analysis of the exact Ollivier-Ricci curvature and the core-periphery partition.

Table 1. Dataset statistics (“m” stands for multi-class classification, and “s” for single-class). In the training graphs, a few isolated nodes with degree zero have been removed.

Dataset	Nodes	Edges	Features	Classes	Train/ Validation/ Test	Training graph	
						Nodes	Edges
CiteSeer	3,327	4,732	500	6 (s)	0.54/0.15/0.31	1,812	1,351
Pubmed	19,717	44,338	500	3 (s)	0.92/0.03/0.05	18,217	37,900
PPI-Large	56,944	818,716	50	121 (m)	0.79/0.11/0.10	44,906	633,198
Ogbn-arxiv	169,343	1,166,243	128	40 (m)	0.54/0.18/0.28	90,941	369,033
Reddit	232,965	11,606,919	602	41 (s)	0.66/0.10/0.24	153,932	5,376,619
Ogbn-products	2,449,026	61,859,140	100	47 (s)	0.08/0.02/0.90	196,615	5,451,633

Note that sample examples in Fig. 2 and curvature comparisons in Fig. 4 and Table 2 only consider the topological structure of subgraphs, thus $\|X(u)\|$ in Eq. (21) and $\|X(u')\|$ in Eq. (23) of our sampler HIS-FF are all set to 1 for $\forall u \in \mathcal{V}_{per}, u' \in \mathcal{V}_{cor}$ in these experiments.

5.2 Chain preservation and curvature maximization

Compared to the supporting role of centrum nodes in shortening the path length between two low-degree nodes, information propagation along consecutive low-degree nodes in a long chain is more effective. Let $\mathcal{P}_G(k)$ denote the set of all chains composed of four nodes with degrees not more than k in the training graph G . Define $\mathbf{1}(\tau \subseteq G_i)$ is 1 if chain τ exists in subgraph G_i , otherwise 0, and let $x \vee y$ denote $\max[x, y]$. Then, we use r_k^n defined in Eq. (24) to measure the preservation rate of the $\mathcal{P}_G(k)$ chains in subgraphs G_i ($i = 1, 2, \dots, n$).

$$r_k^n = \frac{1}{|\mathcal{P}_G(k)|} \sum_{\tau \in \mathcal{P}_G(k)} \bigvee_{i=1}^n \mathbf{1}(\tau \subseteq G_i) \quad (24)$$

Eq. (24) confirms that chain τ is preserved as long as it falls into one of the n subgraphs, since HIS_{G_{CN}s} adopts the loss normalization technique of GraphSAINT that eliminate bias to nodes more

frequently sampled in different subgraphs. As shown in Fig. 5, we compare HIS-FF in **Algorithm 1** with the existing graph samplers introduced in Section 2.2.3 and Fig. 2, which validates the effectiveness in preserving long chains composed entirely of low-degree nodes.

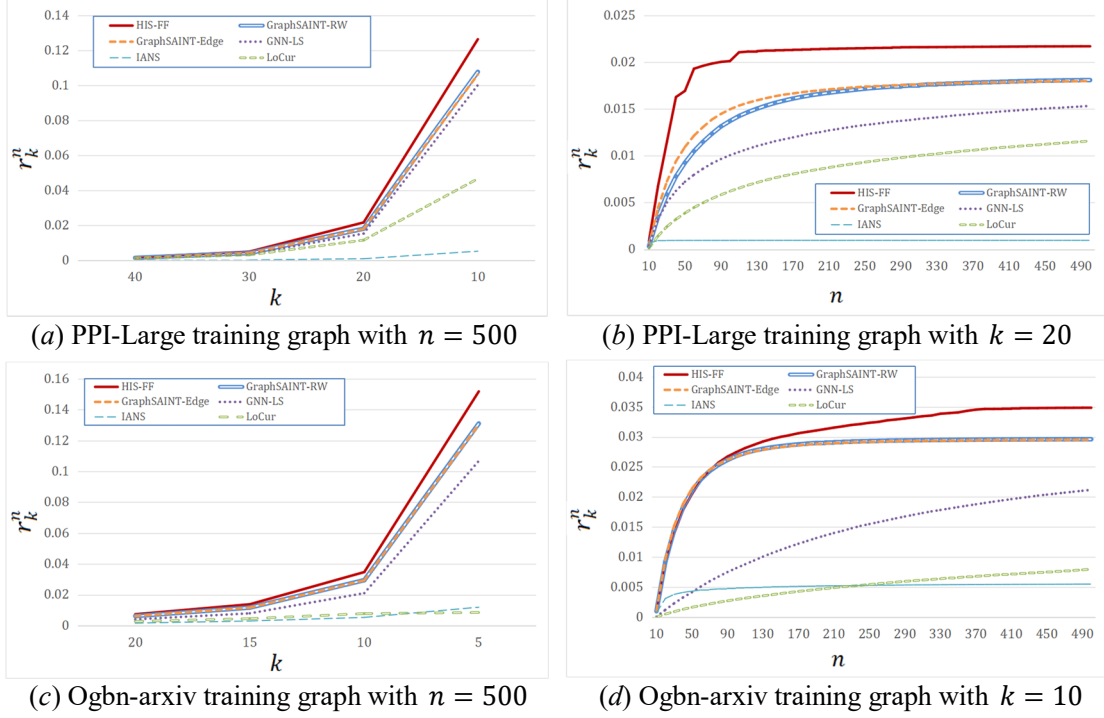


Figure 5. Comparison of preservation rate of chains along low-degree nodes. (a) r_k^n vs. k with $n = 500$ in PPI-Large training graph. (b) r_k^n vs. n with $k = 20$ in PPI-Large training graph. (c) r_k^n vs. k with $n = 500$ in Ogbn-arxiv training graph. (d) r_k^n vs. n with $k = 10$ in Ogbn-arxiv training graph. The measure r_k^n is defined in Eq. (24).

If it is possible to walk along the edges with large curvatures, the distance of node features in the starting and ending nodes of a path can be close [25]. Thus, it is necessary to maximize the curvatures in a subgraph. In 1-hop local structure of the curvatures, the shortest distance between nodes can be obtained by considering only 3-, 4- or 5-cycles for sparse large graphs (see **Appendix A**). As shown in Fig. 2, centrum nodes are critical parts of these cycles and HIS-FF preserves the centrum nodes in most subgraphs. Table 2 shows that HIS-FF can maximize the exact curvature.

Table 2. Comparison of exact Ollivier-Ricci curvature using real-world graphs in [33-35]. Self-loops, multi-edges and edge-direction of the graphs have been removed.

Exact Ollivier-Ricci curvature (see Appendix A)		Average of edge curvatures of 1,000 subgraphs with 10% partial nodes. (The curvature of an edge refers to its curvature on the original graph, not on a subgraph)				Original Graph
		GraphSAINT-Edge	GraphSAINT-RW	LoCur	HIS-FF	
Graphs in [35]	ego-Facebook 4,039 nodes/88,234 edges	0.19	0.22	0.26	0.41	0.32
	CA-GrQc 5,242 nodes/14,484 edges	0.04	0.01	0.05	0.07	0.06
	Wiki-Vote 7,115 nodes/100,762 edges	-0.01	0.05	0.10	0.19	-0.11
	CA-HepTh 9,877 nodes/25,973 edges	-0.30	-0.15	-0.07	-0.06	-0.33
	CA-HepPh 12,008 nodes/118,489 edges	0.11	0.16	0.21	0.56	0.16
In [33]	CiteSeer 3,327 nodes/4,732 edges	-0.03	-0.01	0.01	0.02	-0.24
In [34]	Pubmed 19,717 nodes/44,338 edges	-0.62	-0.45	-0.44	-0.43	-0.61

5.3 Variance reduction for node feature aggregation

Eqs. (9) to (17) allow for a theoretical evaluation of variance in a single-layer GCN. Moreover, the variance in multi-layer GCNs with non-linear activations can be evaluated using experimental methods. Let G_1, G_2, \dots, G_n be n subgraphs obtained by a sampler \mathcal{R} , and $Y_i(v)$ be 2-norm of the feature vector of node v in subgraph $G_i = (\mathcal{V}_i, \mathcal{E}_i)$ after the forward propagation of a full GCN on G_i with the same initialization weight matrix if $v \in \mathcal{V}_i$.

Then, the feature aggregation variance of node v is roughly calculated as follows:

$$\mathbf{Var}(v) = \frac{1}{k} \sum_{j=1}^k \left(Y_{i_j}(v) - \bar{Y}(v) \right)^2 \quad (25)$$

where $Y_{i_1}(v), Y_{i_2}(v), \dots, Y_{i_k}(v)$ are respectively derived by the forward propagation on $G_{i_1}, G_{i_2}, \dots, G_{i_k}$ that are all subgraphs preserving node v , and $\bar{Y}(v) = \frac{1}{k} \sum_{j=1}^k Y_{i_j}(v)$.

In addition, the average value of the feature aggregation variance for all nodes in the training graph $G = (\mathcal{V}, \mathcal{E})$ is calculated as follows:

$$\mathbf{Var}_{\text{avg}} = \frac{\sum_{v \in \mathcal{V}} \mathbf{Var}(v)}{|\mathcal{V}|} \quad (26)$$

The experimental comparison of node aggregation variance is shown in Fig. 6, which verifies that the empirical probability distribution $q(u' | v)$ defined in Eq. (23) does not influence the effectiveness of our method HIS_{GCNs} in variance reduction. Low variance accelerates GCN convergence, thus the experiments on the GCN convergence will be supplemented in Section 5.6.1.

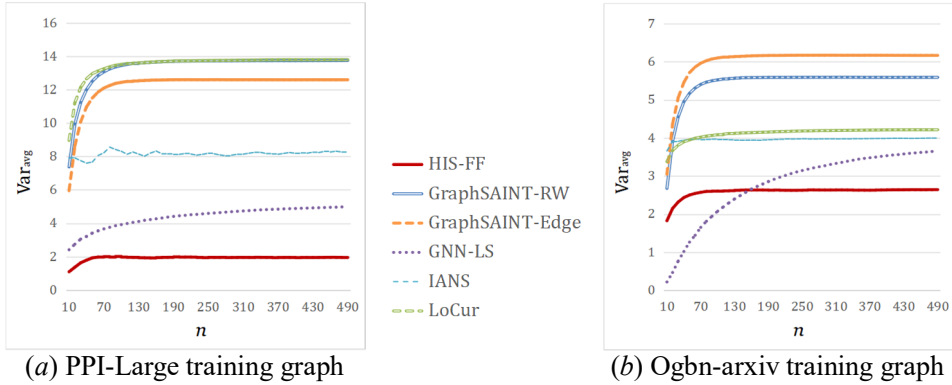


Figure 6. Comparison of node aggregation variance on the same two-layer GraphSAGE model [3]. Sample size (i.e., the number of nodes in subgraphs) was set as 10% partial nodes of the training graphs. (a) $\mathbf{Var}_{\text{avg}}$ vs. n in PPI-Large training graph, where $\mathbf{Var}_{\text{avg}}$ is defined in Eq. (26) and n denotes the number of subgraphs. (b) $\mathbf{Var}_{\text{avg}}$ vs. n in Ogbn-arxiv training graph.

5.4 Settings for node classification tasks

The node classification tasks were tested on the six open datasets described in Table 1. For all datasets, we perform grid search on the hyperparameter space defined by:

- Dropout: $\{0.1, 0.15, 0.2, 0.25, 0.3, 0.4, \dots, 0.8\}$
- Hidden dimension: $\{128, 256, 512\}$
- Learning rate: $\{0.1, 0.02, 0.01, 0.001, 0.0001\}$

For our methods HIS-FF in **Algorithm 1** and HIS-RW in **Algorithm 2**, we use sampling rate η to determine the input sample size $\hat{n} = |\mathcal{V}| \cdot \eta$ where \mathcal{V} is the node set of the training graph, and perform grid search for η and another input parameter γ on the hyperparameter space defined by:

- Sampling rate η : {0.005, 0.01, 0.02, 0.05}
- Parameter γ : {0.1, 0.2, 0.3, ..., 0.8, 0.9, 1.0}

Fig. 7 and Tables 4 to 7 show the convergence and accuracy comparison of various methods. All results correspond to two-layer GNN models. For a given dataset, we keep hidden dimension the same across all methods: the hidden layer dimension is set as 512 for CiteSeer, Pubmed, PPI-Large and Reddit, and 256 for OGBN-Arxiv and OGBN-Products.

For all methods, the optimizer and activation function are Adam and ReLU, respectively. We utilize cross-entropy loss for single-label classification datasets, and binary cross-entropy loss for multi-task datasets. In addition, we sample 100 subgraphs per epoch for all datasets, and the number of epochs is adjusted based on convergence.

Table 3. Training and sampling hyperparameters for HIS_{GCNs}.

Sampler	Dataset	Training		Sampling		
		Learning rate	Dropout	Sampling rate η	Walk length	Parameter γ
HIS-FF	CiteSeer	0.001	0.8	0.01	—	1.0
	Pubmed	0.0001	0.2	0.005	—	1.0
	PPI-Large	0.02	0.1	0.05	—	1.0
	Ogbn-arxiv	0.001	0.3	0.05	—	1.0
	Reddit	0.001	0.15	0.02	—	0.4
	Ogbn-products	0.001	0.3	0.02	—	0.4
HIS-RW	CiteSeer	0.001	0.8	0.01	4	1.0
	Pubmed	0.0001	0.2	0.005	3	1.0
	PPI-Large	0.01	0.1	0.05	15	1.0
	Ogbn-arxiv	0.001	0.3	0.05	2	1.0
	Reddit	0.001	0.15	0.02	4	0.4
	Ogbn-products	0.001	0.3	0.02	2	0.4

The hyperparameters of HIS-FF and HIS-RW are listed in Table 3. In addition, experimental details for core-periphery partition can be found in **Appendix B.1**, experiments for setting parameter γ can be found in **Appendix B.2**, and experiments for setting parameter η can be found in **Appendix B.3**. We first compare sampling-based GCN or GNN methods, including node-wise, layer-wise and subgraph-based samplings, and then focus on the comparison of graph sampling methods within the same GNN architecture. In the former comparison (i.e., Section 5.5), all methods use two-layer GNNs and the same hidden layer dimensions mentioned above, but their other hyperparameters are optimal and obtained by the searching strategies reported in related papers. In the latter comparison (i.e., Section 5.6), the same two-layer GNN model is provided for diverse graph sampling methods, and the model is concretized by GCN [1], GraphSAGE [3] and GAT [36] in sequence. The optimal hyperparameters of the baselines can be found in **Appendix D**.

Moreover, experiments of the samplers on k -layer GNN models with $k \geq 3$ can be found in **Appendix E**. During training on the deep models, we apply DropEdge to alleviate over-smoothing [37] that isolates output representations from input features as model depth increases.

5.5 Comparison of sampling-based GCN or GNN methods

Our methods HIS-FF and HIS-RW are compared with state-of-the-art and open-source methods, including GCN [1], GraphSAGE [3], FastGCN [17], ClusterGCN [20], and SHADOW-SAGE [21], where SHADOW-SAGE is SHADOW-GNN on GraphSAGE model and has two extractors, namely L -hop and Personalized PageRank (PPR)-based [21].

Table 4. Comparison of test set F1-micro score on two-layer GNNs.

Methods	CiteSeer	Pubmed	PPI-Large	Ogbn-arxiv	Reddit	Ogbn-products
GCN	0.711 ± 0.007	0.786 ± 0.002	0.482±0.005	0.702±0.003	0.952±0.004	0.757±0.002
GraphSAGE	0.698 ± 0.006	0.814 ± 0.001	0.618±0.004	0.715±0.003	0.953±0.001	0.760±0.003
FastGCN	0.704 ± 0.015	0.863 ± 0.015	0.507±0.028	0.682±0.043	0.924±0.012	0.744±0.005
ClusterGCN	0.694 ± 0.007	0.882 ± 0.003	0.902±0.002	0.665±0.001	0.954±0.002	0.773±0.001
SHADOW-SAGE (2-hop)	0.726 ± 0.006	0.894 ± 0.001	0.948±0.003	0.715±0.002	0.966±0.001	0.787±0.004
SHADOW-SAGE (PPR)	0.727 ± 0.004	0.896 ± 0.003	0.964±0.002	0.721±0.001	0.967±0.003	0.785±0.003
HIS-FF	0.740 ± 0.007	0.898 ± 0.002	0.985±0.002	0.723±0.001	0.967±0.001	0.788±0.003
HIS-RW	0.728 ± 0.012	0.898 ± 0.002	0.954±0.005	0.722±0.002	0.967±0.002	0.779±0.002

Table 4 compares HIS_{GCNs} (using GraphSAGE model) with various baselines, and the results were obtained by repeating experiments five times. In contrast to the baselines that are capable of learning on arbitrary graphs, including mesh grid, Erdős-Rényi random graphs [26], and power-law graphs [7,8,12], our method HIS_{GCNs} depends on the unique core-periphery structure of scale-free graphs. However, many open standard datasets for node classification are scale-free, such as social network, biological network, citation network, and product information network. Based on the prior topological characteristics of these networks, our samplers HIS-FF and HIS-RW can more easily preserve important information propagation paths in subgraphs with small size, which helps improve the accuracy of node classification.

5.6 Comparison of graph sampling methods

Based on **Algorithms 1 and 2**, our samplers HIS-FF and HIS-RW can be extended to diverse GNN models. Thus, three widely-used GNN models, namely GCN [1], GraphSAGE [3] and GAT [36], are used for comparison, and our samplers are compared with state-of-the-art graph samplers, including GraphSAINT-Edge [6], GraphSAINT-RW [6], LoCur [25], GNN-LS [24], IANS [23], and SLSR [38]. The samplers were tested on the same two-layer GNN model.

5.6.1 Convergence and training time comparison

Fig. 7 shows the convergence and training time comparison of various graph samplers on the same two-layer GraphSAGE model. The training and sampling hyperparameters of the samplers can be found in Table 3 and **Appendix D**.

The training time of Fig. 7 corresponds to GPU execution time that excludes the time for data loading, preprocessing, sampling, validation set evaluation and model saving. The cost of preprocessing and sampling can be found in **Appendix B.1** and **Appendix F**, respectively. All samplers terminate after a certain number of epochs based on convergence.

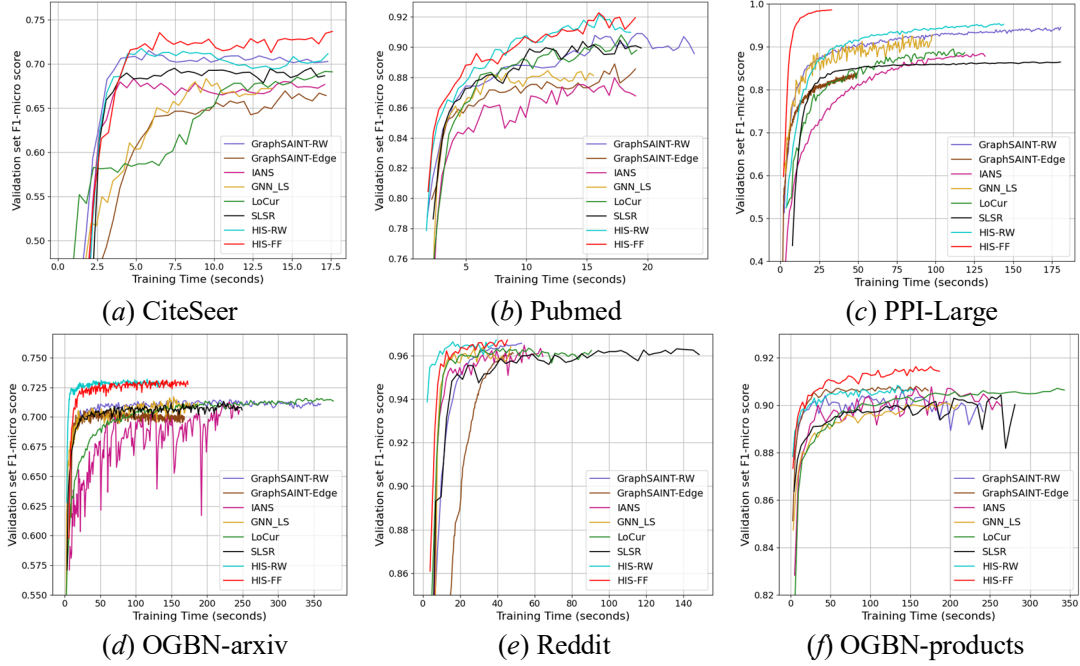


Figure 7. Convergence curves of samplers on the same two-layer GraphSAGE model.

SLSR [38] is a sampler for network crawling and visualization whose goal is to preserve only one subgraph that keeps low variance of degree property and maintains statistical properties of an original graph, such as degree distribution, clustering coefficient and path length distribution. Thus, SLSR takes more time to finely sample the only one subgraph, resulting in the loss of diversity of information propagation chains. Deep graph learning propagates information along important long chains, and expects these chains to appear in at least one of many subgraphs with small size rather than maintaining statistical properties for each subgraph. In addition, SLSR does not consider the variance for node feature aggregation. Therefore, the difference in goals between network crawling (visualization) and deep graph learning results in SLSR not performing well in terms of convergence and accuracy in node classification tasks, as shown in Fig. 7 and Tables 5 to 7.

Existing samplers for graph learning have made significant contributions to the understanding of node aggregation variance and classification accuracy on arbitrary graphs. For scale-free graphs that widely exist in real-world, the role of centrum nodes for deep graph learning is often weakened in theoretical analysis: on the one hand, they are key components in forming 5-cycles (or less) that help shorten the length of propagation paths and maximize the curvature, but on the other hand, their strong interference leads to the loss of massive long chains composed entirely of low-degree nodes, as shown in Fig. 2. Our samplers HIS-FF and HIS-RW 1. maintain the favorable role of the centrum in forming cycles, 2. avoid the unfavorable interference role of the centrum, 3. consider the variance reduction for node feature aggregation, 4. reduce the overhead in subgraph sampling through randomness, and 5. enhance the diversity of long propagation paths in many subgraphs. Although our samplers HIS-FF and HIS-RW are not good at preserving degree distribution of the training graph, they are competent for minibatch learning along propagation paths in scale-free graphs.

Our method HIS_{GCNS} first samples nodes in sparse periphery, and then samples core nodes that are determined by the sampled periphery nodes. The process from periphery to core avoids the high uncertainty of randomly extracting next node from neighbors of a centrum node of the core. In addition, HIS_{GCNS} preserves the centrum to most subgraphs based on **P3**, which helps to control the uncertainty in subgraph structures. Low node aggregation variance in Fig. 6 provides evidence for the fast convergence of our samplers HIS-FF and HIS-RW, as shown in Fig. 7.

5.6.2 Accuracy comparison

Using the same hyperparameters as Section 5.6.1, Tables 5 to 7 show the accuracy comparison of various samplers on GCN, GraphSAGE and GAT models, respectively. The final F1-scores and their confidence intervals were calculated by repeating experiments five times on the same device with the same configurations. The maximum number of epochs for each dataset is pre-set. Specifically, the maximum number is set as 50 for CiteSeer, 100 for Pubmed and Reddit, and 200 for PPI-Large, OGBN-arxiv and OGBN-products. The convergence curves in Fig. 7 were determined by the data obtained after running the maximum number of epochs.

Table 5. Comparison of test set F1-micro score with different samplers on the same two-layer GCN model. Hyperparameters can be found in Table 3 and **Appendix D**.

Samplers	CiteSeer	Pubmed	PPI-Large	Ogbn-arxiv	Reddit	Ogbn-products
GraphSAINT-Edge	0.687 ± 0.007	0.866 ± 0.002	0.834±0.001	0.704±0.002	0.962±0.005	0.755±0.003
GraphSAINT-RW	0.726 ± 0.005	0.877 ± 0.001	0.938±0.005	0.711±0.002	0.966±0.001	0.766±0.003
LoCur	0.702 ± 0.008	0.883 ± 0.003	0.890±0.001	0.709±0.003	0.963±0.002	0.755±0.002
GNN-LS	0.693 ± 0.006	0.859±0.004	0.932±0.008	0.705±0.006	0.965±0.002	0.759±0.005
IANS	0.691 ± 0.015	0.860 ± 0.008	0.873 ± 0.005	0.703±0.003	0.962±0.001	0.774±0.002
SLSR	0.699 ± 0.006	0.873 ± 0.006	0.862±0.003	0.702±0.002	0.960±0.001	0.770±0.004
HIS-FF	0.743 ± 0.008	0.884 ± 0.005	0.965±0.004	0.719±0.003	0.965±0.002	0.781±0.001
HIS-RW	0.735 ± 0.008	0.884 ± 0.004	0.949±0.003	0.716±0.001	0.966±0.001	0.774±0.002

Table 6. Comparison of test set F1-micro score with different samplers on the same two-layer GraphSAGE model.

Samplers	CiteSeer	Pubmed	PPI-Large	Ogbn-arxiv	Reddit	Ogbn-products
GraphSAINT-Edge	0.690 ± 0.008	0.880 ± 0.002	0.839±0.005	0.705±0.004	0.962±0.004	0.760±0.005
GraphSAINT-RW	0.726 ± 0.004	0.891 ± 0.002	0.940±0.001	0.710±0.002	0.966±0.003	0.773±0.002
LoCur	0.708 ± 0.008	0.897 ± 0.003	0.892±0.004	0.711±0.002	0.964±0.001	0.758±0.004
GNN-LS	0.694 ± 0.007	0.873 ± 0.005	0.927±0.008	0.705±0.005	0.964±0.002	0.752±0.007
IANS	0.693 ± 0.018	0.878 ± 0.007	0.884±0.003	0.702±0.002	0.962±0.001	0.774±0.003
SLSR	0.701 ± 0.007	0.888 ± 0.002	0.875±0.004	0.705±0.002	0.962±0.002	0.774±0.004
HIS-FF	0.740 ± 0.007	0.898 ± 0.002	0.985±0.002	0.723±0.001	0.967±0.001	0.788±0.003
HIS-RW	0.728 ± 0.012	0.898 ± 0.002	0.954±0.005	0.722±0.002	0.967±0.002	0.779±0.002

According to Tables 5 to 7, the stable accuracy across different GNN models indicates the high flexibility of all samplers. The datasets in the tables correspond to scale-free networks, thus using prior information unique to these networks can help improve accuracy.

Power law $P(k) \propto k^{-\tau}$ leads to massive low-degree periphery nodes and a small number of high-degree core nodes, and preferential attachment causes the periphery nodes to be densely connected to centrum nodes that are only a few core nodes with top highest-degrees. The degree difference between the centrum and marginal core nodes is usually enlarged in large-scale graphs based on the preferential attachment. Based on BA model [7], edges join a scale-free graph in chronological order. In the process of temporal evolution, a few nodes added to the graph in early stages are more likely to be densely interconnected, forming the prototype of dense core of a large-scale graph. HIS_{G_{CN}s} adopts the unique structure of scale-free graphs resulting from the temporal evolution and preferential attachment. In addition, 1. Since two low-degree nodes are likely to be influential to each other [6], HIS_{G_{CN}s} retains more long chains in periphery, and 2. Since the distance of node features in the starting and ending nodes of a path along high curvature edges is close [25], HIS_{G_{CN}s} preserves the centrum (important for shortening path length and forming cycles) in most subgraphs. Thus, the proposed samplers HIS-FF and HIS-RW perform superior in both accuracy and training time for node classification tasks via minibatch learning.

Table 7. Comparison of test set F1-micro score with different samplers on the same two-layer GAT model.

Samplers	CiteSeer	Pubmed	PPI-Large	Ogbn-arxiv	Reddit	Ogbn-products
GraphSAINT-Edge	0.699 ± 0.005	0.867 ± 0.002	0.840±0.003	0.708±0.002	0.963±0.002	0.756±0.001
GraphSAINT-RW	0.736 ± 0.006	0.884 ± 0.002	0.945±0.002	0.714±0.003	0.966±0.001	0.771±0.002
LoCur	0.715 ± 0.008	0.882 ± 0.002	0.902±0.002	0.710±0.002	0.963±0.001	0.759±0.002
GNN-LS	0.700 ± 0.004	0.853 ± 0.004	0.937±0.005	0.708±0.007	0.965±0.001	0.758±0.004
IANS	0.697 ± 0.018	0.864 ± 0.008	0.858±0.002	0.707±0.002	0.963±0.001	0.776±0.002
SLSR	0.711 ± 0.006	0.874 ± 0.001	0.878±0.003	0.705±0.002	0.963±0.001	0.774±0.003
HIS-FF	0.755 ± 0.005	0.885 ± 0.002	0.979±0.002	0.726±0.002	0.967±0.001	0.789±0.001
HIS-RW	0.748 ± 0.011	0.892 ± 0.001	0.953±0.002	0.721±0.002	0.967±0.003	0.778±0.003

6 Conclusions

Existing subgraph samplers have established a superior foundation for minibatch learning on arbitrary graphs, including mesh grid, Erdős-Rényi random graphs, and power-law graphs. Based on the foundation, we only consider the minibatch learning on scale-free training graphs with power-law degree distribution, since 1. these graphs are abundant in real-world, and 2. a single research object helps to utilize its unique structural information.

Different from subgraph samplers used for network crawling and visualization, we focus on the preservation of critical long chains for information propagation and the reduction of node aggregation variance. Our samplers HIS-FF and HIS-RW cannot maintain the similarity of degree distribution between each subgraph and the training graph, but can maximize the Ollivier-Ricci curvature by preserving numerous and diverse critical long chains that either are not affected by the interference of core nodes or form 5-cycles (or cycles with less edges) through a few centrum nodes.

Using the prior core-periphery structure of scale-free graphs, our method HIS_{G_{CN}s} can preserve important information propagation paths in many small-size subgraphs with fast convergence speed, which helps to improve accuracy and training time via minibatch learning.

References

- [1] Kipf, T. N., & Welling, M. (2016). Semi-supervised classification with graph convolutional networks. *arxiv preprint arxiv:1609.02907*.
- [2] Bai, J., Ren, Y., & Zhang, J. (2021). Ripple walk training: A subgraph-based training framework for large and deep graph neural network. In *2021 International Joint Conference on Neural Networks (IJCNN)* (pp. 1-8). IEEE.
- [3] Hamilton, W., Ying, Z., & Leskovec, J. (2017). Inductive representation learning on large graphs. *Advances in Neural Information Processing Systems* (pp. 1024-1034).
- [4] Serafini, M., & Guan, H. (2021). Scalable graph neural network training: The case for sampling. *ACM SIGOPS Operating Systems Review*, 55(1), pp. 68-76.
- [5] Vatter, J., Mayer, R., & Jacobsen, H. A. (2023). The evolution of distributed systems for graph neural networks and their origin in graph processing and deep learning: A survey. *ACM Computing Surveys*, 56(1), pp. 1-37.
- [6] Zeng, H., Zhou, H., Srivastava, A., Kannan, R., & Prasanna, V. (2020). GraphSAINT: Graph sampling based inductive learning method. In *International conference on learning representations*.
- [7] Barabási, A. L., & Albert, R. (1999). Emergence of scaling in random networks. *Science*, 286(5439), pp. 509-512.
- [8] Kojaku, S., & Masuda, N. (2018). Core-periphery structure requires something else in the network. *New Journal of physics*, 20(4), 043012.
- [9] Kumar, R., Gurugubelli, S., & Chepuri, S. P. (2022). Identifying core-periphery structures using graph neural networks. In *2022 56th Asilomar Conference on Signals, Systems, and Computers* (pp. 251-255). IEEE.
- [10] Gurugubelli, S., & Chepuri, S. P. (2022). Generative models and learning algorithms for core-periphery structured graphs. *arxiv preprint arxiv:2210.01489*.
- [11] Bansal, N., Kaouri, K., & Woolley, T. E. (2025). Reducing size bias in sampling for infectious disease spread on networks. *arxiv preprint arxiv:2501.13195*.
- [12] Jiao, B., Lu, X., Xia, J., Gupta, B. B., Bao, L., & Zhou, Q. (2023). Hierarchical sampling for the visualization of large scale-free graphs. *IEEE Transactions on Visualization and Computer Graphics*, 29(12), pp. 5111-5123.
- [13] Das, S. S., Ferdous, S. M., Halappanavar, M. M., Serra, E., & Pothan, A. (2024). Ags-gnn: Attribute-guided sampling for graph neural networks. In *Proceedings of the 30th ACM SIGKDD Conference on Knowledge Discovery and Data Mining* (pp. 538-549).
- [14] Younesian, T., Daza, D., van Krieken, E., Thanapalasingam, T., & Bloem, P. (2023). Grapes: Learning to sample graphs for scalable graph neural networks. *arxiv preprint arxiv:2310.03399*.
- [15] Ying, R., He, R., Chen, K., Eksombatchai, P., Hamilton, W. L., & Leskovec, J. (2018). Graph convolutional neural networks for web-scale recommender systems. In *Proceedings of the 24th ACM SIGKDD international conference on knowledge discovery & data mining* (pp. 974-983).
- [16] Chen, J., Zhu, J., & Song, L. (2018). Stochastic training of graph convolutional networks with variance reduction. In *International Conference on Machine Learning* (pp. 942-950). PMLR.
- [17] Chen, J., Ma, T., & Xiao, C. (2018). FastGCN: Fast learning with graph convolutional networks via importance sampling. In *International Conference on Learning Representations, ICLR*.
- [18] Huang, W., Zhang, T., Rong, Y., & Huang, J. (2018). Adaptive sampling towards fast graph representation learning. *Advances in Neural Information Processing Systems* (pp. 4558-4567).

- [19] Zou, D., Hu, Z., Wang, Y., Jiang, S., Sun, Y., & Gu, Q. (2019). Layer-dependent importance sampling for training deep and large graph convolutional networks. *Advances in Neural Information Processing Systems* (pp. 11249-11259).
- [20] Chiang, W. L., Liu, X., Si, S., Li, Y., Bengio, S., & Hsieh, C. J. (2019). Cluster-gcn: An efficient algorithm for training deep and large graph convolutional networks. In *Proceedings of the 25th ACM SIGKDD international conference on knowledge discovery & data mining* (pp. 257-266).
- [21] Zeng, H., Zhang, M., Xia, Y., Srivastava, A., Malevich, A., Kannan, R., Prasanna, V., Jin, L., & Chen, R. (2021). Decoupling the depth and scope of graph neural networks. *Advances in Neural Information Processing Systems* (pp. 19665-19679).
- [22] Wan, C., Li, Y., Li, A., Kim, N. S., & Lin, Y. (2022). BNS-GCN: Efficient full-graph training of graph convolutional networks with partition-parallelism and random boundary node sampling. In *Proceedings of Machine Learning and Systems* (pp. 673-693).
- [23] Zhang, Q., Sun, Y., Hu, Y., Wang, S., & Yin, B. (2023). A subgraph sampling method for training large-scale graph convolutional network. *Information Sciences*, 649, 119661.
- [24] Zhao, W., Guo, T., Yu, X., & Han, C. (2023). A learnable sampling method for scalable graph neural networks. *Neural Networks*, 162, pp. 412-424.
- [25] Shu, D. W., Kim, Y., & Kwon, J. (2023). Localized curvature-based combinatorial subgraph sampling for large-scale graphs. *Pattern Recognition*, 139, 109475.
- [26] Erdős, P., & Rényi, A. (1960). On the evolution of random graphs. *Publ. Math. Inst. Hungar. Acad. Sci*, 5, pp. 17-61.
- [27] Qi, X. (2022). A review: Random walk in graph sampling. *arxiv preprint arxiv:2209.13103*.
- [28] Leskovec, J., Kleinberg, J., & Faloutsos, C. (2005). Graphs over time: densification laws, shrinking diameters and possible explanations. In *Proceedings of the eleventh ACM SIGKDD international conference on Knowledge discovery in data mining* (pp. 177-187).
- [29] Yin, H., Shao, Y., Miao, X., Li, Y., & Cui, B. (2022). Scalable graph sampling on gpus with compressed graph. In *Proceedings of the 31st ACM International Conference on Information & Knowledge Management* (pp. 2383-2392).
- [30] Hu, W., Fey, M., Zitnik, M., Dong, Y., Ren, H., Liu, B., Catasta, M., & Leskovec, J. (2020). Open graph benchmark: Datasets for machine learning on graphs. *Advances in Neural Information Processing Systems* (pp. 22118-22133).
- [31] Ollivier, Y. (2009). Ricci curvature of Markov chains on metric spaces. *Journal of Functional Analysis*, 256(3), pp. 810-864.
- [32] Ye, Z., Liu, K. S., Ma, T., Gao, J., & Chen, C. (2019). Curvature graph network. In *International conference on learning representations*.
- [33] Giles, C. L., Bollacker, K. D., & Lawrence, S. (1998). CiteSeer: An automatic citation indexing system. In *Proceedings of the third ACM conference on Digital libraries* (pp. 89-98).
- [34] Yang, Z., Cohen, W., & Salakhudinov, R. (2016). Revisiting semi-supervised learning with graph embeddings. In *International conference on machine learning* (pp. 40-48). PMLR.
- [35] Leskovec, J. (2014). SNAP Datasets: Stanford large network dataset collection. Retrieved February 2025 from <http://snap.stanford.edu/data>.
- [36] Veličković, P., Cucurull, G., Casanova, A., Romero, A., Liò, P., & Bengio, Y. (2018). Graph Attention Networks. In *International Conference on Learning Representations*.
- [37] Rong, Y., Huang, W., Xu, T., & Huang, J. (2020). Dropedge: Towards deep graph convolutional networks on node classification. In *International Conference on Learning Representations*.

[38] Jiao, B. (2024). Sampling unknown large networks restricted by low sampling rates. *Scientific Reports*, 14(1), 13340.

Appendix A: Calculation of the exact Ollivier-Ricci curvature [25,31,32]

Define a random walk μ on a graph $G = (\mathcal{V}, \mathcal{E})$ as a family of probability measure $\mu_v(\cdot)$ on the node set \mathcal{V} for all $v \in \mathcal{V}$. For a node $p \in \mathcal{V}$, the uniform 1-step random walk μ is given by [32]:

$$\mu_v(p) = \begin{cases} \alpha & \text{if } p = v \\ (1 - \alpha)/d_v & \text{if } (p, v) \in \mathcal{E} \\ 0 & \text{otherwise} \end{cases} \quad (27)$$

where \mathcal{E} is the edge set of G , and d_v denotes the degree of node v . We set parameter $\alpha = 0$ that is consistent with the corresponding definition in [25]. Let $d(u, v)$ be the shortest path distance between two nodes u and v , then the Ollivier-Ricci curvature $\kappa(u, v)$ is defined as follows:

$$\kappa(u, v) = 1 - \frac{W_1(\mu_u, \mu_v)}{d(u, v)} \quad (28)$$

where $W_1(\mu_u, \mu_v)$ is the 1-Wasserstein transport distance and is the optimal value of the objective function in the linear optimization problem with $\alpha = 0$:

$$\begin{aligned} & \text{minimize} && \sum_{p \in \mathcal{N}_u} \sum_{q \in \mathcal{N}_v} d(p, q) \pi(p, q) \\ & \text{subject to} && \sum_{p \in \mathcal{N}_u} \pi(p, q) = \frac{1}{d_v} \\ & && \sum_{q \in \mathcal{N}_v} \pi(p, q) = \frac{1}{d_u} \end{aligned} \quad (29)$$

where $\mathcal{N}_u = \{p \in \mathcal{V} | (p, u) \in \mathcal{E}\}$ and $\mathcal{N}_v = \{q \in \mathcal{V} | (q, v) \in \mathcal{E}\}$.

Such a definition captures the behavior that $\kappa(u, v) = 0$ if the random walkers tend to stay at equal distance, $\kappa(u, v) < 0$ if they tend to diverge, and $\kappa(u, v) > 0$ if they tend to converge.

In 1-hop local structure $\{\mathcal{N}_u \cup u\} \cup \{\mathcal{N}_v \cup v\}$ for an edge $(u, v) \in \mathcal{E}$, the distance transported from the neighboring node of u to the neighboring node of v through a 6-cycle is the same as the distance transported through u and v . Thus, the optimal transport distance for the local structure can be obtained by considering 5-cycles or cycles with less edges [25].

Appendix B. 1: Experiments on core-periphery partition [12]

We adopt the core-periphery partition algorithm in [12], since the algorithm only uses a simple graph property, namely node degree, which incurs little overhead in training time. In addition, the algorithm maximizes the number of edges connecting a periphery node and a core node, which helps to minimize the core node ratio (i.e., $|\mathcal{V}_{cor}|/|\mathcal{V}|$) defined as the ratio of the number of core nodes to the total number of nodes in large-scale graphs with power-law degree distribution. The minimization of the core node ratio can enhance the diversity of peripheral chains in many subgraphs, and is helpful in preserving the centrum nodes to most subgraphs.

Our method HIS_{GCNS} only needs to execute the partition algorithm once during preprocessing. Table 8 exhibits the degree threshold, core node ratio and $|\mathcal{E}_{ver}|/|\mathcal{E}|$ obtained by the partition on the training graphs $G = (\mathcal{V}, \mathcal{E})$, where \mathcal{E}_{ver} is defined in Eq. (7) and the number of edges in \mathcal{E}_{ver} can be maximized by Eq. (4). In addition, Table 8 shows the average CPU execution time for five realizations of the core-periphery partition. Using more scale-free graphs extracted from [35], Table 9 further verifies the efficiency of the partition algorithm.

In [12], the degree threshold d_{th} starts from 1 and then grows with steplength 1 until Eq. (4) is satisfied. The test datasets and the optimized code of the core-periphery partition are included in <https://github.com/HuQiaCHN/HIS-GCN>.

Table 8. Core-periphery partition on scale-free training graphs, where d_{th} is the degree threshold, $|\mathcal{V}_{cor}|/|\mathcal{V}|$ is the ratio of the number of core nodes to the total number of nodes, and $|\mathcal{E}_{ver}|/|\mathcal{E}|$ is the ratio of the number of edges in \mathcal{E}_{ver} to the total number of edges.

Training graphs	Nodes	Edges	d_{th}	$ \mathcal{V}_{cor} / \mathcal{V} $	$ \mathcal{E}_{ver} / \mathcal{E} $	Average CPU execution time (s)
CiteSeer	1,812	1,351	2	15.45%	37.23%	0.00
Pubmed	18,217	37,900	8	13.61%	58.90%	0.01
PPI-Large	44,906	633,198	57	12.34%	47.91%	0.03
Ogbn-arxiv	90,941	369,033	23	5.68%	41.50%	0.04
Reddit	153,932	5,376,619	109	16.13%	39.10%	0.59
Ogbn-products	196,615	5,451,633	79	17.72%	47.83%	0.42

Table 9. Core-periphery partition on scale-free graphs in [35]. Self-loops, multi-edges and edge-direction of the graphs have been removed.

Large-scale graphs in [35]	Nodes	Edges	d_{th}	$ \mathcal{V}_{cor} / \mathcal{V} $	$ \mathcal{E}_{ver} / \mathcal{E} $	Average CPU execution time (s)
web-Google	875,713	4,322,051	20	8.60%	55.54%	0.92
com-youtube	1,134,879	2,987,595	39	1.60%	50.92%	2.13
as-skitter	1,696,415	11,095,298	50	2.90%	61.86%	2.28
wiki-topcats	1,791,489	25,444,207	76	5.31%	61.15%	10.51
wiki-Talk	2,394,385	4,659,565	79	0.34%	83.44%	1.71
cit-Patents	3,774,768	16,518,947	13	20.06%	41.35%	0.32

Appendix B. 2: Experiments on parameter γ

Using the same configuration and hyperparameters (except for parameter γ) as those in Table 6, we test the relationship between parameter γ and test set F1-micro score of HIS-FF on two-layer GraphSAGE model. As shown in Table 10, we experimentally set $\gamma = 0.4$ for training graphs that have over 100,000 nodes, otherwise $\gamma = 1$.

Table 10. Relationship between parameter γ and test set F1-micro score of HIS-FF on two-layer GraphSAGE model.

Citeseer training graph with 1,812 nodes		Pubmed training graph with 18,217 nodes		PPI-Large training graph with 44,906 nodes		Ogbn-arxiv training graph with 90,941 nodes		Reddit training graph with 153,932 nodes		Ogbn-products training graph with 196,615 nodes	
γ	Test F1-score	γ	Test F1-score	γ	Test F1-score	γ	Test F1-score	γ	Test F1-score	γ	Test F1-score
0.2	0.737±0.002	0.2	0.897±0.003	0.2	0.825±0.001	0.2	0.715±0.003	0.2	0.965±0.001	0.2	0.784±0.003
0.4	0.735±0.003	0.4	0.896±0.005	0.4	0.954±0.003	0.4	0.718±0.004	0.4	0.967±0.001	0.4	0.788±0.003
0.6	0.739±0.002	0.6	0.895±0.004	0.6	0.970±0.002	0.6	0.719±0.001	0.6	0.966±0.002	0.6	0.784±0.001
0.8	0.734±0.003	0.8	0.895±0.003	0.8	0.977±0.003	0.8	0.722±0.002	0.8	0.963±0.002	0.8	0.781±0.001
1	0.740±0.007	1	0.898±0.002	1	0.985±0.002	1	0.723±0.001	1	0.962±0.001	1	0.777±0.002

Appendix B. 3: Experiments on sampling rate η

Using the same configuration and hyperparameters (except for sampling rate η) as those in Table 6, we test the relationship among sampling rate η , test set F1-micro score, and training time of HIS-FF on the same two-layer GraphSAGE model. As shown in Fig. 8, except for CiteSeer (small-scale dataset), with increasing η , the test F1-score slightly decreases after reaching its peak, while the training time continues to increase. We observe that the test F1-score peak corresponds to low sampling rates, thus our method HIS_{GCNs} is capable of minibatch learning with small size.

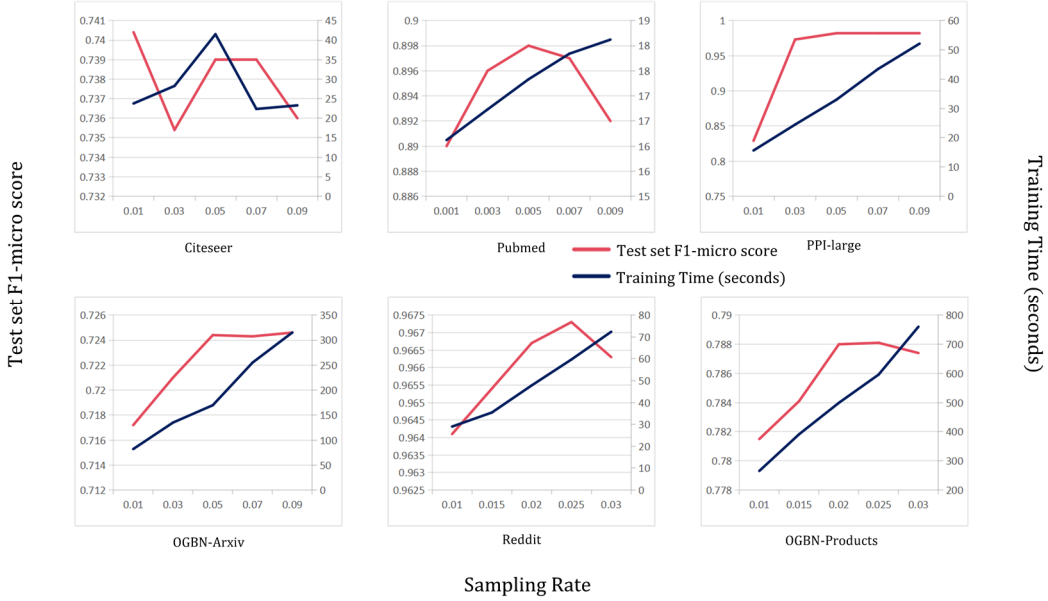


Figure 8. Relationship among sampling rate η , test set F1-micro score, and training time (seconds) of HIS-FF on the same two-layer GraphSAGE model and five different datasets.

Appendix C: HIS_{GCNs} training algorithm

Algorithm 3: HIS_{GCNs} training algorithm

Input: Scale-free training graph $G = (\mathcal{V}, \mathcal{E}, X)$; Labels \bar{Y} ; Sampler SAMPLE (HIS-FF or HIS-RW).

Output: GCN model with trained weights.

- 1: Pre-processing: Setup SAMPLE parameters; Core-periphery partition [12]; Compute normalization coefficient λ [6].
 - 2: **For** each minibatch **do**
 - 3: $G_{sub} = (\mathcal{V}_{sub}, \mathcal{E}_{sub}) \leftarrow$ Sampled subgraph of G according to SAMPLE.
 - 4: GCN construction on G_{sub} .
 - 5: $\{y_v | v \in \mathcal{V}_{sub}\} \leftarrow$ Forward propagation of $\{x_v | v \in \mathcal{V}_{sub}\}$.
 - 6: Backward propagation from λ -normalized loss $L(y_v, \bar{y}_v)$ [6]. Update weights.
 - 7: **End for**
-

Algorithm 3 illustrates the training algorithm of our method HIS_{GCNs}.

Appendix D: Training and sampling hyperparameters for baselines

Training and sampling hyperparameters of baselines are illustrated in Table 11. The number of subgraphs used for training is determined by the number of epochs that has been illustrated in Section 5.6.2, and therefore not listed in Table 11.

Table 11. Training and sampling hyperparameters for baselines.
The number of nodes in subgraphs can be determined by sampling rate η .

Sampler	Dataset	Training		Sampling						
		Learning rate	Dropout	Sampling rate η	Edge budget	Roots	Walk length	Steps	Cluster number	Neighbor sampling ratio
GraphSAINT-Edge	CiteSeer	0.001	0.8	—	10	—	—	—	—	—
	Pubmed	0.0001	0.2	—	80	—	—	—	—	—
	PPI-Large	0.01	0.1	—	1600	—	—	—	—	—
	Ogbn-arxiv	0.001	0.3	—	2600	—	—	—	—	—
	Reddit	0.001	0.1	—	6000	—	—	—	—	—
	Ogbn-products	0.001	0.3	—	2800	—	—	—	—	—
GraphSAINT-RW	CiteSeer	0.001	0.8	—	—	5	4	—	—	—
	Pubmed	0.0001	0.2	—	—	25	3	—	—	—
	PPI-Large	0.01	0.1	—	—	1000	4	—	—	—
	Ogbn-arxiv	0.001	0.3	—	—	1250	2	—	—	—
	Reddit	0.001	0.1	—	—	2000	4	—	—	—
	Ogbn-products	0.001	0.3	—	—	1250	2	—	—	—
LoCur	CiteSeer	0.001	0.8	0.01	—	—	—	4	—	—
	Pubmed	0.0001	0.2	0.005	—	—	—	3	—	—
	PPI-Large	0.02	0.1	0.05	—	—	—	4	—	—
	Ogbn-arxiv	0.001	0.3	0.05	—	—	—	3	—	—
	Reddit	0.001	0.1	0.02	—	—	—	3	—	—
	Ogbn-products	0.001	0.3	0.02	—	—	—	3	—	—
GNN-LS	CiteSeer	0.001	0.8	0.01	—	—	—	—	—	—
	Pubmed	0.0001	0.2	0.005	—	—	—	—	—	—
	PPI-Large	0.02	0.1	0.05	—	—	—	—	—	—
	Ogbn-arxiv	0.001	0.3	0.05	—	—	—	—	—	—
	Reddit	0.001	0.1	0.02	—	—	—	—	—	—
	Ogbn-products	0.001	0.3	0.02	—	—	—	—	—	—
IANS	CiteSeer	0.001	0.8	0.01	—	—	—	—	5	0.5
	Pubmed	0.0001	0.2	0.005	—	—	—	—	10	0.5
	PPI-Large	0.01	0.3	0.05	—	—	—	—	15	0.5
	Ogbn-arxiv	0.001	0.3	0.05	—	—	—	—	10	0.5
	Reddit	0.001	0.1	0.02	—	—	—	—	10	0.5
	Ogbn-products	0.001	0.3	0.02	—	—	—	—	45	0.5
SLSR	CiteSeer	0.001	0.8	0.01	—	—	—	—	—	—
	Pubmed	0.0001	0.2	0.005	—	—	—	—	—	—
	PPI-Large	0.02	0.1	0.05	—	—	—	—	—	—
	Ogbn-arxiv	0.001	0.3	0.05	—	—	—	—	—	—
	Reddit	0.001	0.1	0.02	—	—	—	—	—	—
	Ogbn-products	0.001	0.3	0.02	—	—	—	—	—	—

Appendix E: Experiments on k -layer GNN models with $k \geq 3$

We use the GraphSAGE model for the experiments in Table 12 and Fig. 9. During training on the k -layer models with $k \geq 3$, we apply DropEdge [37] to both the baselines and HIS_{GNNs} models. DropEdge helps improve accuracy by alleviating over-smoothing.

Table 12. Comparison of test set F1-micro score on the same 3-layer GraphSAGE model (tuned with DropEdge).

Samplers	CiteSeer	Pubmed	PPI-Large	Ogbn-arxiv	Reddit	Ogbn-products
GraphSAINT-Edge	0.724 ± 0.006	0.898 ± 0.002	0.834 ± 0.001	0.705 ± 0.002	0.964 ± 0.005	0.766 ± 0.002
GraphSAINT-RW	0.731 ± 0.003	0.899 ± 0.004	0.943 ± 0.002	0.714 ± 0.002	0.967 ± 0.001	0.789 ± 0.005
LoCur	0.721 ± 0.008	0.894 ± 0.003	0.904 ± 0.004	0.713 ± 0.004	0.964 ± 0.003	0.773 ± 0.003
GNN-LS	0.730 ± 0.004	0.882 ± 0.004	0.934 ± 0.008	0.707 ± 0.005	0.965 ± 0.001	0.758 ± 0.004
IANS	0.710 ± 0.015	0.873 ± 0.005	0.925 ± 0.005	0.705 ± 0.004	0.963 ± 0.001	0.785 ± 0.002
HIS-FF	0.747 ± 0.009	0.902 ± 0.005	0.989 ± 0.004	0.732 ± 0.003	0.967 ± 0.002	0.794 ± 0.003
HIS-RW	0.740 ± 0.006	0.896 ± 0.004	0.974 ± 0.003	0.729 ± 0.001	0.968 ± 0.001	0.792 ± 0.002

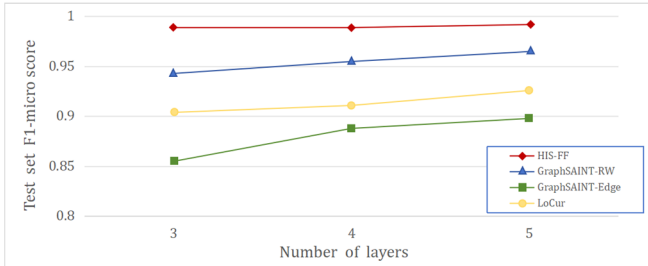


Figure 9. Comparison of test set F1-micro score on PPI-Large as model depth increases (tuned with DropEdge), with hidden layer dimension 512 and parameters in Tables 3 and 11.

Appendix F: Cost of graph samplers

Graph sampling introduces little training overhead. Let t_s be the average CPU time to sample one subgraph, and let t_t be the average GPU time to perform the forward and backward propagation on one minibatch on the two-layer GraphSAGE model. The average time corresponds to 100 realizations. Fig. 10 shows the ratio t_s/t_t for various datasets. The parameters of the samplers are listed in Tables 3 and **Appendix D**, and none of the samplers adopt parallel strategies.

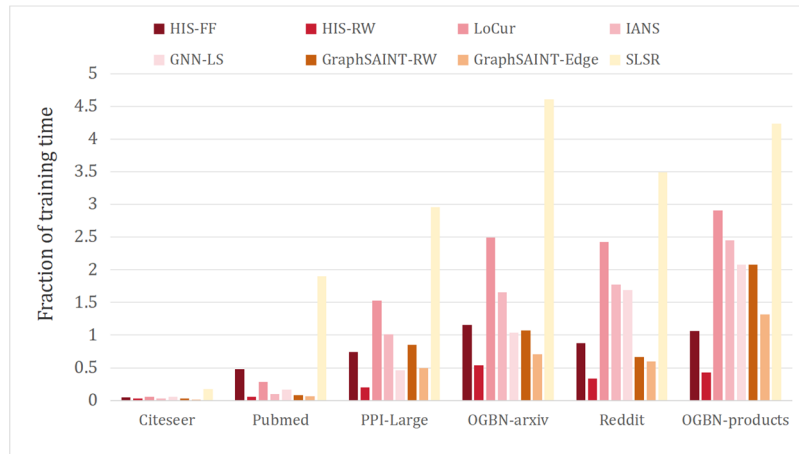


Figure 10. Fraction of training time (i.e., the ratio t_s/t_t) on sampling.

CRedit authorship contribution statement:

Qia Hu: Software; Data curation; Methodology; Formal analysis;
Writing - Original draft.

Bo Jiao: Conceptualization; Methodology; Formal analysis; Supervision;
Writing - Review & Editing.

Corresponding author: Bo Jiao (jiaobleetc@outlook.com)